UAB

Universitat Autònoma de Barcelona

Maximum Power Point Tracking of Photovoltaic system using Non-Linear Controllers

Hina Gohar Ali

Supervisor: Professor Ramon Vilanova

Ph.D. Programme in Electrical Engineering and Telecommunications
Department of Telecommunications and Systems Engineering
Autonomous University of Barcelona

This thesis is submitted for the degree of
Ph.D. in Telecommunications and Systems Engineering

School of Engineering   November 2020

Dr. Ramón Vilanova i Arbós, professor at Universitat Autònoma de Barcelona,

CERTIFIES:

That the doctoral thesis entitled "**Maximum power point tracking of photovoltaic system using non-linear controllers**" by Hina Gohar Ali, presented in partial fulfillment of the requirements for the degree of Doctor in Telecommunications and Systems Engineering of Department of Telecommunications and Systems Engineering, has been developed and written under his supervision.

Dr. Ramón Vilanova i Arbós   Hina Gohar Ali

Director   Ph.D. Candidate

Bellaterra, August 2020.

Acknowledgements

First of all, I would like to express my deep gratitude and appreciation to my thesis supervisor, Professor Dr. Ramon Vilanova i Arbos, for his invaluable support, expert guidance and comments during my PhD study. His patience and enthusiasm has encouraged me a lot to overcome the most difficult time and complete this final phase. He gave me full moral support to continue my research work in the moments of despondency and leaving the assignment. I pay my special cordial thanks to my previous advisor Dr. Asier Ibeas who not only administrated my research activities in the start, but also guided and encouraged my innovative ideas until I was working with him. I would must mention Prof. Gary Junkin the previous Doctorate students coordinator for his support, discussion and resolving my Ph.D. admission matters when I was at very critical stage and indecisive in continuation of my research studies at UAB.

I would like further to say my cordial thanks to my funding institute in my country to National University of Sciences and Technology (NUST) Islamabad, Pakistan for awarding me funding for my Doctorate studies in Spain under faculty development program. I am very thankful to Engr Kamran Akhtar (Deputy Director NUST HRD) for his kindness and facilitating me time to time during my studies in abroad. I would pay special cordial thanks to Dr. Ammar Hassan (Local Supervisor) from School of Electrical Engineering Computer Science (SEECS), NUST for his accessibility, responding to my emails and monitoring my research progress. Also I would say thanks to Principle SEECS Dr. Osman Hasan and Senior Head of Department Dr. Hassaan Khaliq Qureshi for their contribution in following up my research progress. I am thankful to Prof. Dr. S. M. Hassan Zaidi and Dr. Farid Gul who were present at the time of my final interview with Pro-Rector Academic NUST before departing to Spain in March 2017.

Throughout the PhD course, fortunately I had an opportunity to co-work with Prof. Jorge Aurelio Herrera, Andrés Tobón, and Dr. Julián Peláez-Restrepo under the Santander research mobility performed in UTADEO Bogota-Colombia during spring semester 2019; part of my research projects which inspired the study cases in this thesis. I would like to express my deep gratitude to Prof. Dr. V. M. Istemihan Genc for providing research stay opportunity in his researh group at Istanbul Technical University, Department of Electrical Engineering

I would like to dedicate this thesis to my loving parents Gohar Ali my father and Safina Gul my mother and my academic supervisor Dr. Ramón Vilanova who guided and inspired me in this process and to my mentor.

Abstract

The increasing energy demands, depleting fossil fuels and increasing global warming due to carbon emission has arisen the need for an alternate, overall efficient and environment-friendly energy system. Solar energy is considered to be one of the most inexhaustible form of energy in this universe, but it has the problem of low efficiency due to varying environmental conditions. Solar panel exhibits nonlinear behaviour under real climatic conditions and output power fluctuates with the variation in solar irradiance and temperature. Changing weather conditions and nonlinear behavior of PV systems pose a challenge in tracking of varying maximum power point. Hence, to continuously extract and deliver the maximum possible power from the PV system, under given environmental conditions, the maximum power point tracking (MPPT) control strategy needs to be formulated that continuously operates the PV system at its MPP. A robust nonlinear controller is required to ensure MPPT by handling nonlinearities of a system and making it robust against changing environmental conditions. Sliding mode control (SMC) is extensively used in non-linear control systems and has been implemented in photovoltaic systems (PVSs) to track MPP. SMC is robust against disturbances, model uncertainties and parametric variations. It depicts undesirable phenomenon like chattering, inherent in it causing power and heat losses. In this thesis, first an integer order SMC controller is formulated for extracting maximum power from a solar PV system under variable climatic conditions employing the perturb and observe (P&O) MPPT scheme for the proposed stand-alone PV system. The proposed system consists of two loops schemes, namely the searching loop and the tracking loop. P&O MPPT is utilized in the searching loop to generate the reference signal and a tracking SMC controller is utilized in the other loop to extract the maximum PV power. PV system is connected with load through the power electronic DC-DC boost converter. A mathematical model of the boost converter is derived first, and based on the derived model, a SMC is formulated to control the gate pulses of the boost converter switch. The closed loop system stability is verified through the Lyapunov stability theorem. The proposed control scheme is tested under varying irradiance levels and the simulation results are compared with the classical proportional integral derivative (PID) controller. Classical SMC depicts undesirable phenomenon like chattering, inherent in it causing power and heat losses. In the next part of this thesis, the

design of adaptive sliding mode controller (ASMC) is discussed for the proposed PV system. The adopted control is executed utilizing an ASMC and the enhancement is actualized utilizing an Improved Pattern Search Method (IPSM) MPPT optimization algorithm. An IPSM MPPT is used to generate the reference voltage in order to command the underlying ASMC controller. Comparison with two other optimization algorithms, namely, a Perturb & Observe (P&O) and Particle Swarm Optimization (PSO) with IPSM for MPPT has been conducted. As a non-linear strategy, the stability of the adaptive controller is guaranteed by conducting a Lyapunov analysis. The performance of the proposed control architectures is validated by comparing the proposals with that of the well-known and widely used PID controller. The simulation results validate that the proposed controller effectively improves the voltage tracking, system power with reduced chattering effect and steady-state error. A tabular comparison is provided at the end of each optimization algorithms category as a resume quantitative comparison. It is anticipated that this work will serve as a reference and provides important insight into MPPT control of the PV systems.

Table of contents

List of figures

List of tables

Abbreviations

PV	Photovoltaic
DC	Direct Current
AC	Alternating Current
MPP	Maximum Power Point
MPPT	Maximum Power Point Tracking
CTs	Conventional Techniques
SCTs	Soft Computing Technique
P&O	Perturb and Observe
INC	Incremental Conductance
AITs	Artifical Intelligence Techniques
BITs	Bio-Inspired Techniques
FL	Fuzzy Logic
ANN	Artifical Neural Network
GA	Genetic Algorithm
PSO	Particle Swarm Optimization
GPSM	Generalized Pattern Search Method
IPSM	Improved Pattern Search Method
SMC	Sliding Mode Control
ASMC	Adaptive Sliding Mode Control
PID	Proportional Integral Derivative
VSC	Variable Structure Control
VSCS	Variable Structure Control System
MIMO	Multiple Input Multiple Output
SMPS	Switched Mode Power Supply
PSIM	PowerSim
IAE	Integral Absolute Error

Chapter 1

Introduction

1.1 Motivation

Energy production is a challenge of great importance for the future. Energy market has witnessed significant changes regarding to the consumption of renewable energy and fossil fuel resources. This is due the raising awareness of environmental damages, the limited nature of fossil fuel supplies, the political and economical pressure of many countries as well as the growing investments of green energy [1]. Today, much of the world's energy production comes from fossil fuels. The consumption of these resources results in greenhouse gas emissions which increase pollution. At the same time, an excessive consumption reduces the reserves of this type of energy. Due to the increasing fuel prices and related environmental concerns, renewable energies become an important source to supply electricity to buildings and industrial sectors [2]. Renewable energy sources play an important role in electric power generation. Wind, hydro, geothermal, and solar energies have been available since the birth of our planet and have been used by the first human generation in different ways. The main advantage of these renewable energies is that their use reduces pollution and production of greenhouse gases such as carbon dioxide and nitrogen oxides that are responsible for global warming [3]. Nowadays, the exploitation of these energies knows a remarkable taking profit from the accelerated technological advances. Solar energy is considered among the fast-developing technologies and experiences a considerable drop in equipment costs [4].

Photovoltaic technology (PV) is an essential technology that can convert solar energy into electrical energy directly by using photovoltaic panel. A photovoltaic system converts light into electrical direct current by taking advantage of the photoelectric effect. The photovoltaic power systems are generally classified according to their functional and operational requirements, their component configurations, and how the equipment is connected to other power sources and electrical loads [5]. The two principal classifications are grid-connected

systems and stand-alone systems. Grid-connected PV system [6] is an electricity generating solar PV system that is connected to the utility grid. It is composed of solar panels, one or several inverters, a power conditioning unit and grid connection equipment. Stand-alone PV systems [7] are designed to operate independent of the electric utility grid, and are generally designed and sized to supply certain DC and/or AC electrical loads.

Photovoltaic solar energy suffers from the problem of maximization the transfer of power photovoltaic generator to the load. This is due to the nonlinear nature of the electrical characteristics (V–I) of PV cells. These characteristics depend on the environmental conditions such as temperature and solar irradiation characteristics which vary with the solar irradiance and temperature of the cell. Efficiency becomes low in PV due to the energy transformation from electrical to solar, which causes the main obstacles in the maximum solar energy utilization. Consequently, it is of great importance to obtain the maximum efficiency of PV systems. In order to increase the power output of a photovoltaic system, it is necessary to force the photovoltaic panel to work in maximum power point (MPP). Therefore, maximum power point tracking (MPPT) techniques are introduced to extract maximum power from PV panels to significantly use the PV panel power [8–10].

A number of MPPT techniques are available in literature. Numerous algorithms on MPPT have been developed and studied which are different from one another based on various different features such as system convergence speed, complexity level, the required sensors, effectiveness range, cost, method of implementation, hardware requirements and some other aspects [11]. Generally, these algorithm techniques are divided into Conventional Techniques (CTs), Soft Computing Technique (SCTs), linear and nonlinear control techniques [12]. In Conventional algorithms Perturb and Observe (P&O) [13], and Incremental Conductance (INC) [14] are the main basic algorithms. These proposed CTs techniques are simple, easy in implementation and have the capacity of tracking the MPP efficiently at present ecological conditions, but the drawback of these CTs is the fluctuations around MPP which influences the accuracy rapidity of the system resulting in a loss of useful power [15]. Techniques based on Soft-computing have presented a powerful tool to deal with MPPT optimization when compared to the conventional ones [16]. SCTs techniques consist of Artificial Intelligence Techniques (AITs) [17] and Bio-Inspired Techniques (BITs) [18] . Fuzzy logic [19], artificial neural network [20] and genetic algorithms [21] comes in the category of AITs. These methods require extensive high computation when dealing with the nonlinear characteristics of the I-V curves although AITs methods are effective generally. Alongwith this, the PV system operating conditions change continuously with time therefore, MPPT has to respond in real time to the environmental condition variations (insolation and temperature). Hence, a large memory size and computing requirements are usually required. The BITs technqiues

are proposed in literature which ensure the optimal searching ability without performing excessive mathematical calculations. These methods have the tendency to converge quickly to a global maximum; thus can save power loss even in a partially shaded environment. Cuckoo search algorithm [22], ant colony optimization [23], particle swarm optimization (PSO) [24] and evolutionary algorithm [25] are the proposed latest techniqiues developed in the class of BITs. Despite their usefulness in various environmental conditions, these techniques are inefficient because of their slow convergence obstruct their practical usage as on-line solutions. Recently, a MPPT improvement approach dependent on Pattern Search was proposed in [26]. The strategy introduced depends on Generalized Pattern Search Method (GPSM). The GPSM was proposed in [27] for subsidiary free unconstrained enhancement of constantly differentiable convex function and has been utilized from that point forward in various control approaches. In addition, Improved Pattern Search Method (IPSM) optimization algorithm is introduced in [28]. The main advantage of IPSM with respect to the previous discussed is that the pool search guarantees that the global maximum is attained in all cases and this fact is tackled in this paper by means of theoretical convergence results.

The non-linear characteristics of the output PV system make it necessary to obtain the MPP operation. For this purpose, in this thesis we present the developing and modeling of the sliding mode controller (SMC) employing P&O, PSO and IPSM MPPT schemes. SMC is used in photovoltaic system to obtain MPP due to the non-linear feature of PV and power converters. It is a non-linear controller which has gained a lot of attraction in the designing of nonlinear control systems due to its simplicity, robustness, good dynamic behavior [29]. Two-loop MPPT approach is utilized in which the controller track the reference signal generates by MPPT schemes under rapidly changing atmosperhic conditions. Asymptotic stability of the whole system is verified using Lyapunov stability criteria.

Moreover, one more contribution have been made to the MPPT procedures in this thesis. We further present analysis of adaptive sliding mode (ASMC) in comparison with classical sliding mode controller to address the chattering phenomenon present in classical SMC. Therefore, to eliminate the chattering effect in classical SMC controller, ASMC is formulated with a two-loop control approach for the extraction of maximum power from a PV panel under varying climatic conditions. P&O, PSO and IPSM optimization MPPT algorithms are employed to generate the reference signal for the ASMC control law. In short, the controller objective would be to keep tracking of the reference voltage(s) employing by MPPT schemes and to obtain maximum power from PV with high performance.

1.2   Aim of this thesis

The following aims are defined for the development of this thesis:

- Review of the state of the art on MPPT optimization schemes.

- Identifying optimization methodologies and MPPT-based controllers needed to extract the MPP.

- Selection of the MPPT schemes to be implemented and reference signal generation by employing P&O, PSO and IPSM optimization algorithms.

- Design nonlinear sliding mode controller based on system dynamics and converter mathematical model.

- Validate the performance of the developed controller for the proposed stand-alone PV system and compare its performance with classical PID controller.

- Introduce adaptive sliding mode controller for the same system to remove chattering presents in sliding mode controller behaviour and enhance the overall system's dynamic response.

1.3   Structure of the Thesis

This thesis is divided in four parts and the contents are organized as follows:

Part I: Fundamentals 1
In this first part, the aim is to introduce the background of the solar photovoltaic system and the description of different components use in PV system.

Chapter 2: Provides theoretical details about solar panel, discussion of single diode model & two diode model representation of solar panel, show power electronic DC-DC converters working topology & operating modes model and overview of MPPT optimization techniques.

Chapter 3: In this chapter, basic control principle and theoretical background of SMC is presented. Some design examples of nonlinear system are shown using SMC controller. Design examples of the SMC controller for the nonlinear system are developed and stability is proved. Simulation results of the system are obtained in Matlab showing robustness of the SMC. Further Adaptive SMC controller is developed which is designed for another nonlinear plant exmaple and stability is checked by Lyaunov function. Simulation results are displayed in Matlab.

Part II: Contribution of SMC and Adaptive SMC in MPPT problem

In this second part of the thesis, the idea is to discuss non-linear controllers which will be used in this study. Modeling of SMC and Adaptive SMC controllers will be shown for the proposed PV system in this work to deal with the MPPT problem.

Chapter 4: This chapter begins with the introduction of one loop and two loop control schemes which are used for the MPP tracking controller. Description of different components of the proposed PV system are discussed which are used in this work. PV panel two diode model is presented with the boost converter and load. P&O, PSO and IPSM MPPT optimization algorithms are explained for the generation of the reference signal which is required to controller for tracking the voltage signals. Hereafter, SMC is derived based on boost converter mathematical model and controller is formulated to generate output signal to the converter switches. Stability proof of the SMC is ensured. Next, the design of adaptive SMC is introduced for the proposed PV system to deal with chattering and high frequency oscillations. Control law is formulated using DC-DC converter dynamics and an appropriate sliding surface is chosen. Adpative SMC is derived and stability is proved by Lyapunov.

Part III: SMC and Adaptive SMC application with different MPPT schemes

In this third part, the results of SMC and Adaptive SMC controllers will be shown with different MPPT schemes. PID results will be discussed too to show comparative analysis of all controllers.

Chapter 5: This chapter provides the simulations results obtained by SMC controller with P&O MPPT scheme under environmental conditions. First results are shown with PID controller in terms of voltage tracking, tracking error and PV panel power. After that, the results are shown with SMC controller. Lastly, comparative analysis is provided in tabular form for both controllers to show the performance characteristics of the conventional controller and the proposed controller.

Chapter 6: This chapter deals the results obtained using Adaptive SMC controller employing P&O, PSO and IPSM MPPTs. Results are shown and discussed of the conventional PID controller and the proposed Adaptive SMC controller with each MPPT schemes. Discussion is provided at the end of the all obtained simulated results. Performance characteristics parameters are presented under discussion section in tabular form in terms of overshoot, response time and power losses. The tables provide the different considered figures of merit. Integral absolute error (IAE) performance index is determined also to depict the controller performance.

Part IV: Conclusions and perspectives
A final part summarizes the conclusions of the thesis and the proposal for future work.
Chapter 7: finally, the conclusions and main contributions are pointed out, also some
future work and research to be conducted are presented.

1.4   Contributions of this research

The work leading to this thesis has been presented in different scientific publications as well
as in a number of project deliverable reports. Following are the list of contributions:

JOURNAL

1. **H.Gohar Ali**, R. Vilanova Arbos, J. Herrera, A. Tobón, and J. Peláez-Restrepo, "Non-
   linear sliding mode controller for photovoltaic panels with maximum power point
   tracking," in *Processes*, vol. 8, no. 1, January 2020.

1. **H.Gohar Ali**, R. Vilanova Arbos, "Chattering Free Adaptive Sliding Mode Controller
   For Photovoltaic Panels with Maximum Power Point Tracking," published in *Special
   Issue Energies MDPI* (Selected Papers from 20 IEEE International Conference on
   Environment and Electrical Engineering (EEEIC 2020), vol. 13. no. 21, October 2020.

CONFERENCE

1. **H. Gohar Ali**, J. Herrera, R. Vilanova Arbos, "Perturb & Observe based Integer
   Order Sliding Mode MPPT Control of Solar Photovoltaic," published in *International
   Conference on Automation Control Engineering Computer Science*, Turkey, October
   2019.

1. **H. Gohar Ali**, R. Vilanova Arbos, and J. Peláez-Restrepo, "Perturb & Observe based
   Adaptive Sliding Mode MPPT Control of Solar Photovoltaic System," published in
   *2020 IEEE International Conference on Environment and Electrical Engineering and
   2020 IEEE Industrial and Commercial Power Systems Europe (EEEIC / ICPS Europe)*,
   Madrid, Spain, October 2019.

Part I

Fundamentals

Chapter 2

Photovoltaic System

2.1 Introduction

The increasing political and environmental problems related to the fossil fuel are the main drawbacks of solar energy source exploitation. A way to overcome these difficulties and to satisfy the growing electricity demand around the world is the use of photovoltaic systems which allow converting solar energy into electricity from sunlight. A photovoltaic system or a PV system is a power system designed to supply usable solar power by means of photovoltaics. It consists of an arrangement of several components, including solar panels to absorb and convert sunlight into electricity, power electronic DC-DC converters to interface between PV panels and loads for MPPT controller, a solar inverter to convert the output from direct to alternating current and other electrical accessories to set up a working system. Photovoltaic energy sources can be used as stand-alone systems and grid-connected systems (see Fig. 2.1) and their applications include water pumping, battery charging, home power supplies, street lighting, refrigeration, swimming-pool heating systems, hybrid vehicles, telecommunications, military space and satellite power systems, and hydrogen production.

2.2 Modeling of solar PV

A PV system directly converts sunlight into electricity. Solar cell is the main component of a PV system which are grouped to form PV panels or arrays. It is the basic power conversion of a solar system and its working principle is based on the ability of semiconductors to convert light directly into electricity by generation of charge carriers. A solar cell is basically a diode. Incident light generates electron hole pair which results in generation of electric current. Several solar cells are combined to form bigger units called solar panels which are further
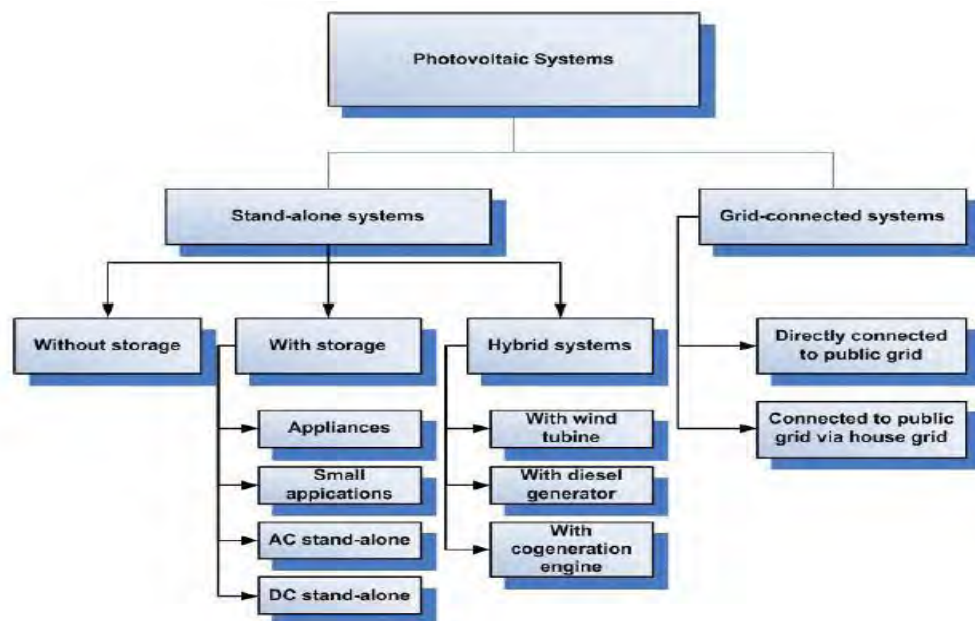
Fig. 2.1 Applications of PV systems.

interconnected in parallel/series combination to obtain required voltage, current and power. For simplicity in analyzing characteristics of solar cells, electrical equivalent circuits are realized and are hence modelled using simulation softwares. It helps in predicting behavior under various environmental conditions, and further in obtaining (I-V) and (P-V) characteristic curves. The common approach is to utilize the electrical equivalent circuit, which is primarily based on a light generated current source connected in parallel to a p-n junction diode. Many models have been proposed for the simulation of a solar cell or for a complete photovoltaic (PV) system at various solar intensities and temperature conditions. The key factor that affects the results of the simulation and accuracy in representing the nonlinear characteristics of the PV system is modeling. To exhibit the nonlinear characteristics of the PV system, there are different types of models mentioned in several literatures in the last few years like single-diode model, double-diode model, three-diode model, and much more. The single-diode model and double-diode model are the most common models used due to their ease of implementation [30]. For precise PV cell modeling and better accuracy, in this work, we use a two diode PV model which involves identification of more parameters at the expense of longer computational time and is known as being a seven-parameter model. Simulations are based on the double-diode model, since their estimation is more useful with other models (i.e., single diode model)[31]. The PV panel based on the two diode model is shown in Fig.2.2. The equivalent circuit of photovoltaic panel based on two-diode model consists of a series resistor (R_s), shunt resistor (R_p), two diodes in anti-parallel and a current
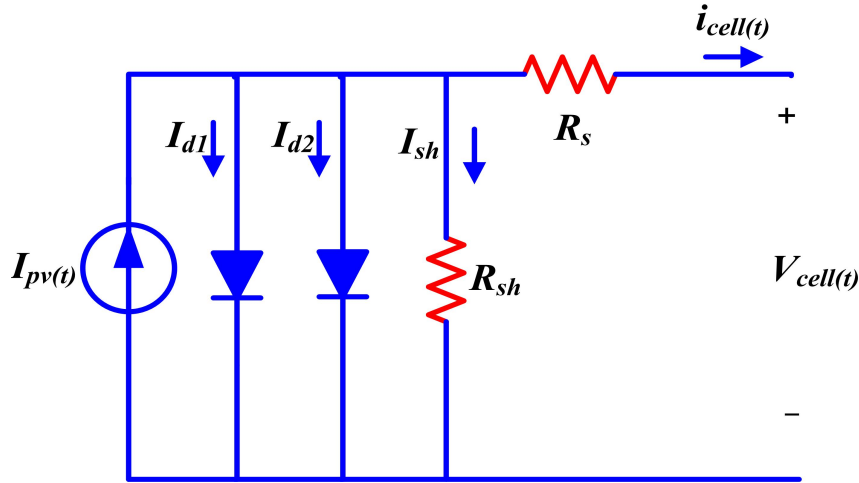
Fig. 2.2 Photovoltaic (PV) panel double-diode model representation.

source. Two-diode model takes into the consideration of recombination effect by including second diode in parallel with the single cell model. It is basically the modified form of single diode model. The following characteristic Eq. 2.1 shows the solar panel current and voltage relationship.

$$I = I_{ph} - I_{o1}\left(e^{\frac{V+IR_S}{N_{s1}V_T}} - 1\right) - I_{o2}\left(e^{\frac{V+IR_S}{N_{s2}V_T}} - 1\right) - \frac{V+IR_S}{R_p} \tag{2.1}$$

In Eq. 2.1, V & I are the voltage and output current of solar cell, I_{ph} is the light generated current, I_s is the reverse saturation current of the diode, (N_{s1} & N_{s2}) are the number of cells in series, (I_{o1} & I_{o2}) the diodes saturation current, V_T is thermal voltage equivalent while R_s and R_p is the series and shunt resistances respectively. The electrical output characteristics of the PV module are plotted in Fig.2.3 by applying the mathematical model of the PV described in Eq. 2.1. From these figures, it can be noticed that the PV module has nonlinear characteristic which varies with solar irradiance and temperature. Under a specific light intensity or temperature condition, the output power will monotonically increase and then monotonically decrease as the voltage increases. There is a different point in each curve at which the maximum power is produced by the module. To solve this problem a MPPT controller is used. Power electronic DC-DC converter selection and designing is the major target in MPPT system to run the PV module at its MPP.
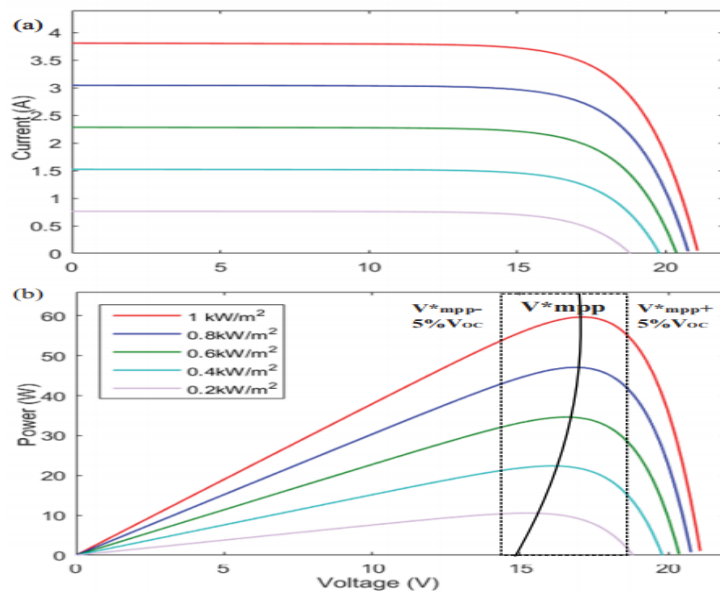
Fig. 2.3 PV module characteristic curves at various radiance: (a) I-V curve (b) P-V curve.

2.3   DC-DC Converter

In the I-V and P-V characterisitic of a PV, it is important to mention that there exist a unique operating point marked as MPP in I-V and P-V curve for varying irradiation and temperature. At the same time this MPP point keeps shifting its position when any atmospheric change occurs. Since per watt cost of solar PV and installation cost are higher; it forced PV system to operate the PV panel at MPP. Thus MPPT controllers are designed to keep tracking MPP and they form an integral part of PV system. One of the best ways of implementing MPPT controller is by introduction of power electronic DC-DC converter interface between PV source and load. Therefore, to operate the PV panel at MPP a DC-DC converter controlled by the MPPT is inserted between the PV panel and the load as shown in Fig. 2.4. DC-DC converter is a device that converts a DC voltage from one level to another level. DC-DC converter can be used in switching mode controllers to change unregulated DC voltage into a regulated DC output voltage. These converters are controlled by switching power device. For low-power applications, MOSFETs can be used, but IGBTs are preferred for utility scale applications. Each active and passive elements are energized and de-energized by controlling the power switching device with a proper pulse-width modulated (PWM) signal. To generate a PWM signal and control the converters, duty cycle must be determined. The regulation is typically accomplished by PWM at a fixed frequency and variable duty cycle. BJT, MOSFET, or IGBT are normally used as switching devices. DC-DC converters play an important role in the maximum power point tracking process. As by connecting the array's output terminals
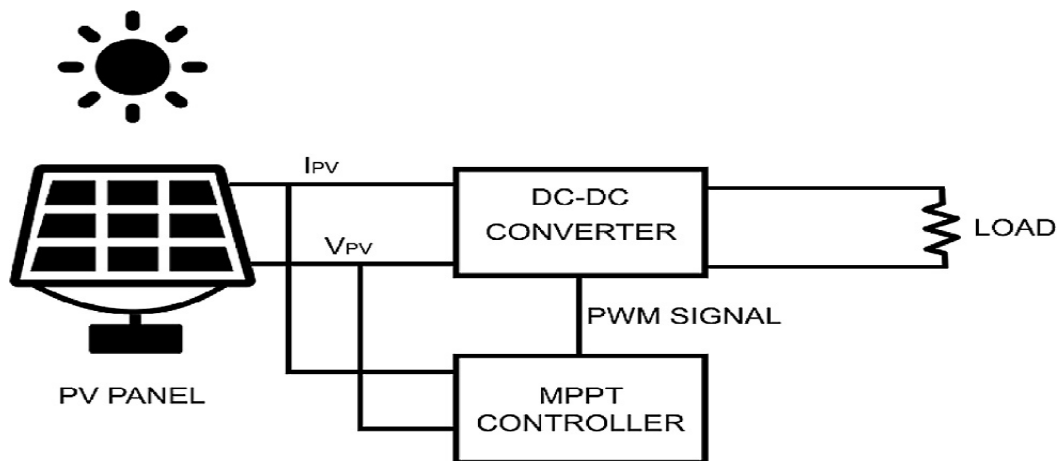
Fig. 2.4 Block diagram of MPPT.

with the DC-DC converter's input terminals, the array voltage can be controlled by varying the duty cycle of the converter and the voltage at which maximum power is obtained can be maintained. There are four fundamental topologies of switching controllers [32].

1. Buck converter

2. Boost converter

3. Buck-boost converter

4. C´uk converter

Among these four converters only the buck and the boost are the basic converter topologies while other converters are combinations of the two basic topologies.

2.3.1 Boost converter design

Boost converter is a DC-DC converter with an output voltage greater than the input. It increases input voltage to a desired voltage level at the output. It is a class of Switched-mode power supply (SMPS) that contains, at least, two semiconductors (diodes or transistors) and one energy storage element (inductor or capacitor). The basic circuit is shown in Fig. 2.5. The input voltage source is connected to an inductor. The solid-state device which operates as a switch is connected across the source. The second switch used is a diode. The diode is connected to a capacitor, and the load and the two are connected in parallel. The inductor connected to input source leads to a constant input current, thus the Boost converter is seen as the constant current input source. The controlled switch is turned on and off by using Pulse Width Modulation (PWM). PWM can be time-based or frequency based. Frequency-based modulation has disadvantages like a wide range of frequencies to achieve the desired control

of the switch which in turn will give the desired output voltage. Time-based modulation is mostly used for DC-DC converters. The frequency remains constant in this type of PWM modulation. The operating principle of a boost converter consists in two stages depending on
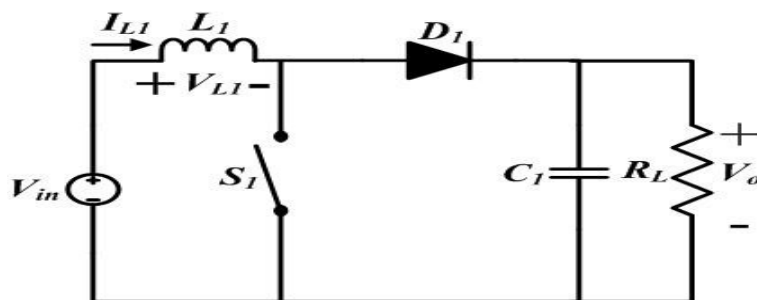
Fig. 2.5 Boost converter.

the state of the switch. The ON state of the switch during the period of T_{on} and the OFF state of the switch during the turns off T_{off} time period. In general, it has two modes of operation. The first mode is when the switch is ON and conducting.

Mode I: Switch is ON, Diode is OFF

The switch is ON and therefore represents a short circuit ideally offering zero resistance to the flow of current so when the switch is ON all the current will flow through the switch and back to the DC input source. The switch is ON for a time T_{on} and is OFF for a time T_{off}. We define the time period, T as $T = T_{ON} + T_{OFF}$ and the switching frequency,

$$f_{switching} = \frac{1}{T} \tag{2.2}$$

Now define another term i.e. the duty cycle,

$$D = \frac{T_{ON}}{T} \tag{2.3}$$

Next is to analyze the Boost converter in steady state operation using KVL.

$$V_{in} = V_{L_1} \tag{2.4}$$

$$V_{L_1} = L_1 \frac{dI_{L_1}}{dt} = V_{in} \tag{2.5}$$

$$\frac{dI_{L_1}}{dt} = \frac{\Delta i_{L_1}}{\Delta t} = \frac{\Delta i_{L_1}}{DT} = \frac{V_{in}}{L_1} \tag{2.6}$$

Since the switch is closed for a time $T_{ON} = D_T$ we can say that $\Delta t = DT$.

$$(\Delta i_{L_1})_{closed} = \left(\frac{V_{in}}{L_1}\right) DT \qquad (2.7)$$

Mode II: Switch is OFF, Diode is ON

In this mode, the polarity of the inductor is reversed. The energy stored in the inductor is released and is ultimately dissipated in the load resistance, and this helps to maintain the flow of current in the same direction through the load and also step-up the output voltage as the inductor is now also acting as a source in conjunction with the input source.

$$V_{in} = V_{L_1} + V_o \qquad (2.8)$$

$$V_{L_1} = L\frac{di_{L_1}}{dt} = V_{in} - V_o \qquad (2.9)$$

$$\frac{di_{L_1}}{dt} = \frac{\Delta i_{L_1}}{(1-D)T} = \frac{V_{in} - V_o}{L_1} \qquad (2.10)$$

Since the switch is open for a time $T_{off} = T - T_{ON} = T - DT = (1-D)T$ we can say that $\Delta t = (1-D)T$ It is already established that the new change of the inductor current over any one complete cycle is zero.

$$(\Delta i_{L_1})_{closed} + (\Delta i_{L_1})_{open} = 0 \qquad (2.11)$$

$$\left(\frac{V_{in} - V_o}{L_1}\right)(1-D)T + \left(\frac{-V_o}{L_1}\right)DT = 0 \qquad (2.12)$$

$$\frac{V_o}{V_{in}} = \frac{1}{1-D} \qquad (2.13)$$

'D' is the duty cycle varies between 0 and 1. From the above equation it can be seen that if 'D=1' then the ratio of output voltage to input voltage at steady state goes to infinity, which is not physically possible.Therefore, to remove the maximum power of a panel, a control strategy is implemented, which handles the duty cycle and always manages to extract the maximum possible power of the panel. For this work, the boost topology has been chosen.

2.4   Maximum Power Point Tracking Algorithms

Maximum power point tracking (MPPT) is a significant component in a photovoltaic system that allows to draw out the utmost maximal power from PV at a maximum power point (MPP)

[33]. As mentioned in 2.2, the irradiation and temperature affect the PV output power. These atmospheric conditions are not constant during a single day. This causes the MPP to move depending on the temperature and irradiation conditions. Great power losses occur when the operating point is not close to ensure that the maximum available power is obtained from the PV panel. Therefore, MPPT algorithms are necessary in PV applications and the use of MPPT algorithms is required in order to obtain the maximum power from a solar array. This means that there is always one optimum terminal voltage for the PV array to operate at with each condition as shown in Fig. 2.6, to obtain the maximum power out of it i.e. increase the array's efficiency. This point depends mainly on irradiance and temperature. The location of the MPP is unknown, but can be located, either through search algorithms or by calculation models.
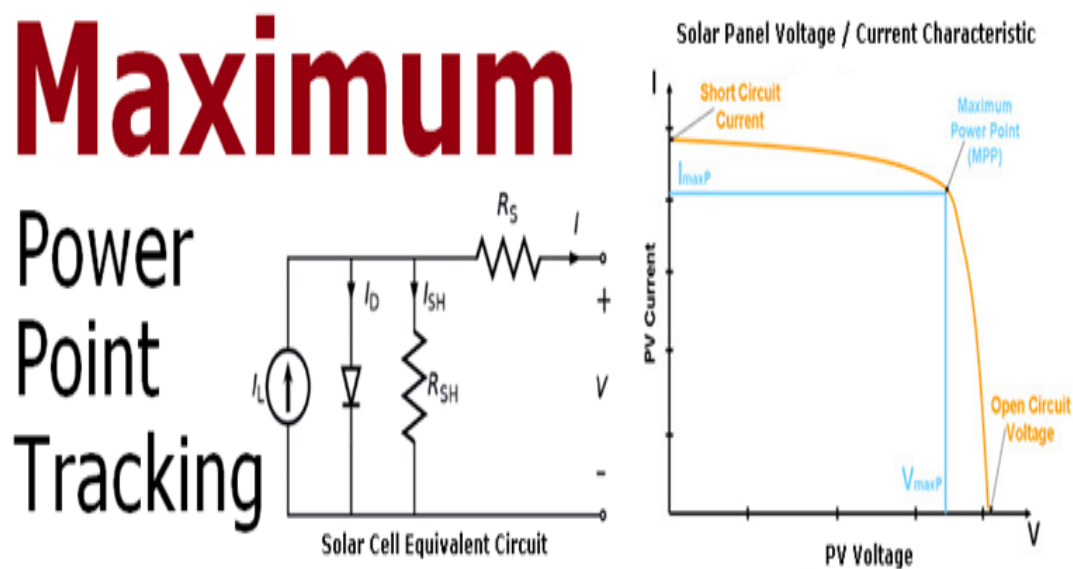
Fig. 2.6 PV curve showing Maximum power point

MPP tracking techniques consist in adjusting the output voltage of the PV to extract the maximum available power at any change in the input (temperature, irradiance). A critical review of various MPPT techniques reported in literature to handle uniform and partial shaded conditions are reported in the following section.

2.5 Conventional methods

2.5.1 Perturb and observe

One of the most popular methods used for maximum power point tracking in solar PV is Perturb and Observe (P&O) method. In this method, based on sensor inputs the PV power is calculated and the voltage perturbations are introduced to deduct the direction of tracking. According to the voltage perturbation the output power may either continuously rise or fall. Thus, the algorithm continuously keeps tracking the MPP via voltage perturbations; hence it oscillates around the vicinity of MPP [34].A simple P&O algorithm implementation is shown in Fig. 2.7. Even though, the method has less complexity in comparison to other MPPT algorithms, it is not preferred in high power applications.
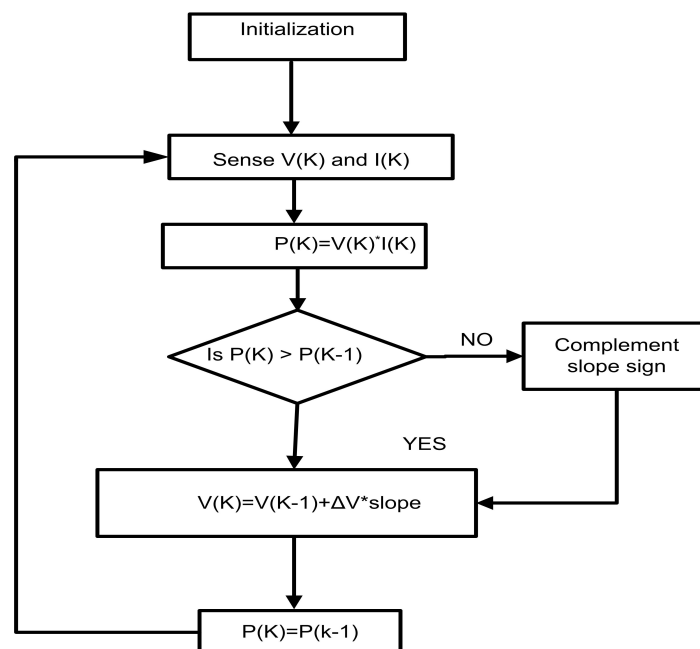
Fig. 2.7 Simple P&O algorithm.

It is a well known fact that P&O is suffered due to repeated perturbations and power oscillations; numerous techniques on improving the perturbation rate for performance enhancement are reported [35–37]. Therefore, modified techniques of P&O are formulated in literature. Conventional P&O method is one of the most used methods in practice and by the majority of authors [38]. This method is based on the trial and error process in finding and tracking the MPP. At every cycle, the tracking controller measures the PV current and voltage and deduces the actual PV power, then perturbs the operating point by sweeping the operating voltage and monitoring the variation of power. If the power increases, the

next perturbation of the operating voltage should be in the same direction. However, if the power decreases, the operating voltage is perturbed in the opposite direction. This scenario is repeated until reaching the MPP. The maximum point is reached when $\frac{dP_{PV}}{dV_{PV}} = 0$. The conventional flowchart of this modified P&O algorithm is shown in Fig. 2.8. Different P&O approaches developed in implementation of MPPT. It can be inferred that, to handle the problem of power fluctuation around the vicinity of MPP; various research articles attempted in improving the performance of P&O method.
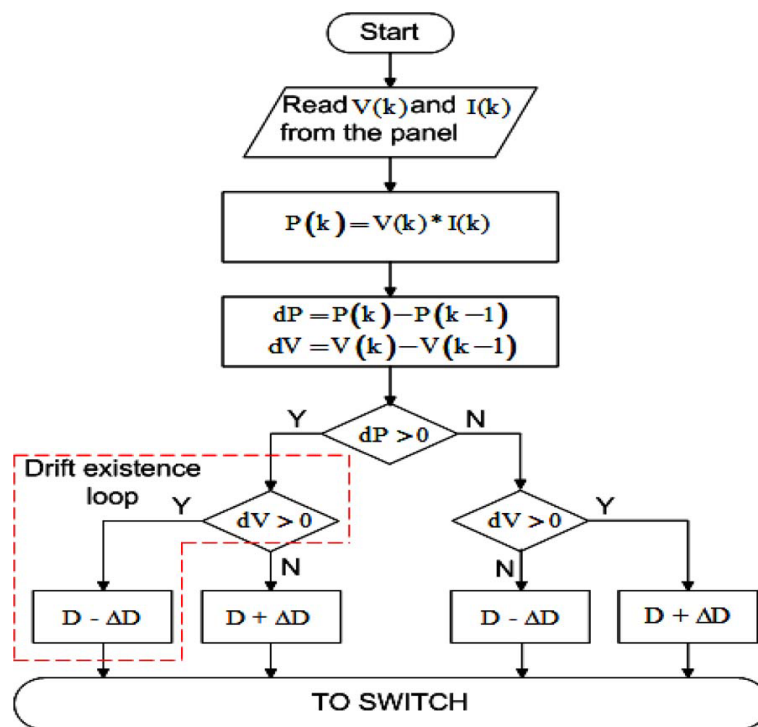
Fig. 2.8 Conventional P&O algorithm flowchart.

2.5.2 Incremental Conductance algorithm

To track MPP, Incremental Conductance (INC) method utilizes the ratio of incremental conductance to instantaneous conductance value of the PV module. Based on this value, the slope of P-V characteristics is altered. In reference to the change in slope, duty cycle for converter is generated [39, 40]. For MPP tracking applying INC algorithm follows three common steps:

1. When $\frac{dP_{PV}}{dV_{PV}} = 0$, the error is zero and V_{mp} can be achieved.

2. When $\frac{dP}{dV} > 0$, (i.e.,) $\frac{dP}{dV} > -\frac{I}{V}$, the MPP is dragged towards the left of the curve (error is positive)

3. When $\frac{dP}{dV} < 0$, (i.e.,) $\frac{dP}{dV} < -\frac{I}{V}$, the MPP is dragged towards the right of the curve (error is negative)

The flowchart for simple INC method is shown in Fig. 2.9. The researchers have followed many techniques to reduce the tracking error in INC method.
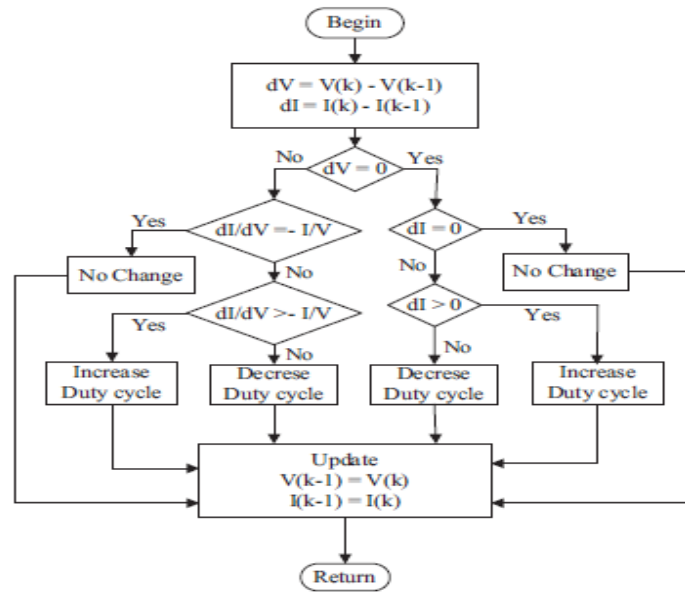
Fig. 2.9 Incremental conductance algorithm flowchart.

2.5.3   Hill climbing algorithm

Hill Climbing technique is one of the oldest classical methods used for Maximum power point tracking. It is widely used due to its simplicity and effectiveness [41]. In this method, the voltage and current values are sensed and based on the calculated power, the duty cycle of the converter is appropriately adjusted [42]. The duty cycle is either incremented or decremented. So, that after a certain number of cycles, the converter is able to reach MPP duty cycle. This technique is lucid, easy to understand and implement. The flowchart of the HC method is shown in Fig. 2.10. The major drawback of this method is that increased oscillations are noticed near the optimum operating point corresponding to the maximum extractable power i.e., it fails to converge at MPP, and the time taken to reach steady state depends on the value of initial duty cycle and step size.
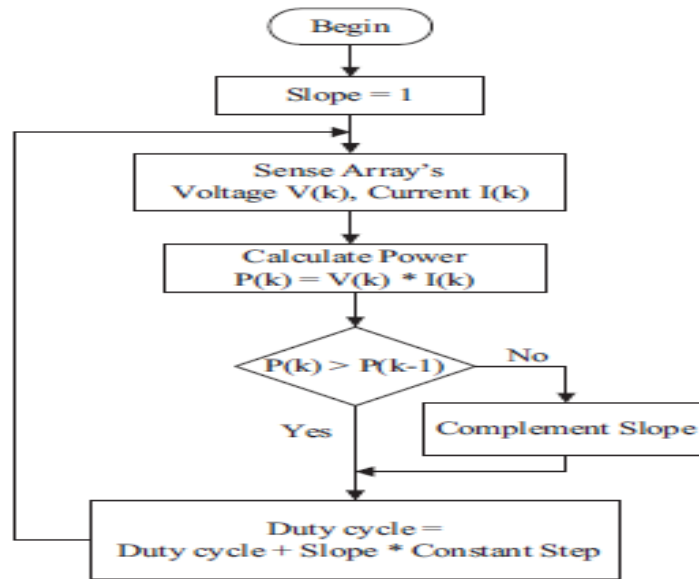
Fig. 2.10 Flowchart for hill climbing algorithm.

2.6   Soft computing techniques

Over the last decade, soft computing techniques are the prime choice in solving non-linear problems. These techniques assure high reliability and faster convergence. Because of the certain inherent drawbacks present in conventional methods various soft computing algorithms have been proposed for the implementation of MPPT. The following section corners a detailed survey and analysis on different soft computing techniques that have been successfully employed for maximum power extraction.

2.6.1   Fuzzy Logic

The Fuzzy Logic (FL) is a rule based algorithm with robustness to solve non-linear optimization problem. Because of advantages like (i) Flexible operation, (ii) Convenient user interface, (iii) Ease of implementation and (iv) Qualified validation, the Fuzzy method is preferred in implementation for MPPT. However, it is less seen that FL is implemented alone; but, it is highly appreciated when used in combination with other algorithms like artificial neural network [11], Genetic algorithm and other conventional methods [43]. FL method follows three steps like fuzzification, inference fuzzy rules and defuzzification for its MPP tracking. In these steps, Fuzzy inference and designing of fuzzy rules decides the optimal performance of the system. But then, to design Fuzzy rules abundant knowledge and high amount of training is needed.

2.6.2 Artifical Neural Network

Artificial Neural Network is a technique derived from the behavior of neurons. Since it is an algorithm of artificial intelligence, ANN has the ability to think of its own. But then, much knowledge is needed to train the neurons present in the algorithm [44, 45]. From the survey, it is very obvious that ANN involves three layers in MPPT installation. A typical three layer ANN model is shown in Fig. 2.11. Due to its enlarged optimization scope, the ANN is preferred to implement in combination with other conventional MPPT techniques to extract maximum power from a PV array [46, 47].
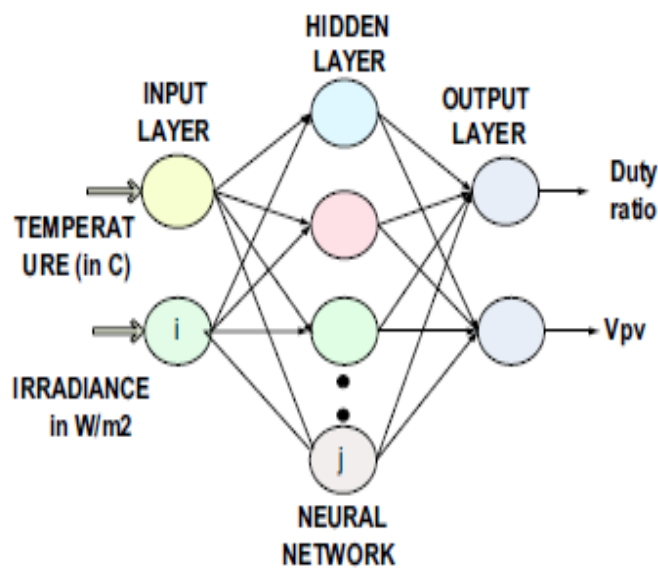
Fig. 2.11 Three layer ANN.

2.6.3 Genetic algorithm

Genetic algorithm is one of the prime preferences for researchers when wide stochastic search is needed. For instance, GA is applied widely in many applications and few of its implementation are: (i) remanufacturing process planning and scheduling [48], (ii) power grid wind disaster management [49], (iii) collaborative product customization [50] and (iv) Fuel flow- rate in transport aircraft [51]. Since the PV systems under partial shaded conditions exhibit multiple peaks; it is highly challenging to track the global maximum point. Hence a wide search is needed to get solution for this non-linear problem. Because of the diversity in solution GA is preferred for solar MPPT [52].

2.6.4 Particle Swarm Optimization

The potential of Particle Swarm Optimization has made it as an excellent choice for non-linear optimization problems. PSO method derives its search ability from the behavior of flocks, swarms and insects [53]. Over the past decade, PSO is seen one of the most preferred optimization technique for MPPT application. The inherent idea behind PSO is that the initial particles are chosen randomly inside the boundary limits. These particles/duty cycles are made to move in search space. The best movement in the initial values is known as P_{best} and the overall best in next iterations is known as G_{best}. Further, the velocity and position of the particles are updated every iteration and the process is con- tinued until the best position is reached. The movement of PSO particles in random search space is shown in Fig. 4.6. The position and velocity update is given in Eqs. 2.14 and 2.15
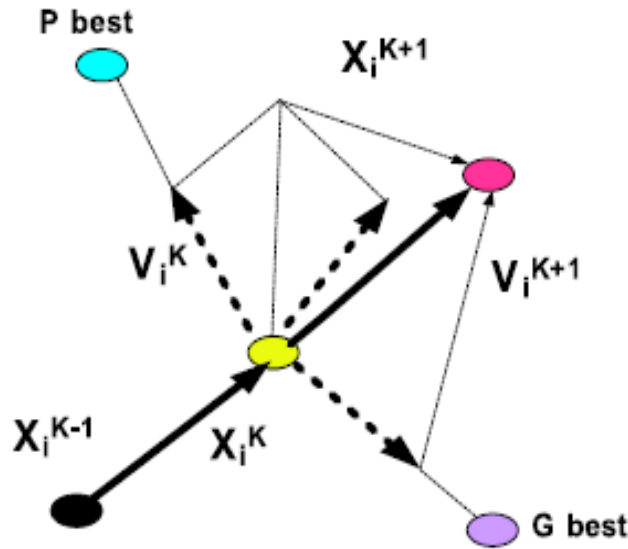
Fig. 2.12 Movement of particles in search space for PSO method.

$$X_i^{t+1} = X_i^t + V_i^{t+1} \tag{2.14}$$

$$V_i^{t+1} = WV_i^t + 1 + C_1 rand()(P_{besti}^t - X_i^t) + C_2 rand()(g_{besti}^t - X_i^t) \tag{2.15}$$

where 'W' is the inertia weight, 'X' corresponds to position, 'V' corresponds to velocity, 'C_1' and 'C_2' are inertia constants and 't' corresponds to iteration count.

Chapter 3

Sliding Mode Control (SMC) Theory

This chapter is based on basic sliding mode control principle and design. Sliding mode techniques are one approach to solving control problems and are an area of increasing interest.

3.1 SMC Background

One of the methods used to solve control problems are the sliding mode techniques. These techniques are generating greater interest. A set of robust control methods have been developed to eliminate any discrepancy. One such approach to the robust control controller design is called the sliding mode control (SMC) methodology. This is a specific type of variable structure control system (VSCS). In the early 1950s, Emelyanov and several co-researchers such as Utkins and Itkis [54] from the Soviet Union, proposed and elaborated the variable structure control (VSC) with generated significant interest in the control research community. SMC has been applied into general design method being examined for wide spectrum of system types including non-linear system, multi-input multi-output (MIMO) systems, discrete-time models, large-scale and infinite-dimension systems, and stochastic systems. The most eminent feature of SMC is that it is completely insensitive to parametric uncertainty and external disturbances during sliding mode [55]. VSC utilizes a high-speed switching control law to achieve two objectives. Firstly, it drives the nonlinear plant's state trajectory onto a specified and userchosen surface in the state space which is called the sliding or switching surface. This surface is called the switching surface because a control path has one gain if the state trajectory of the plant is "above" the surface and a different gain if the trajectory drops "below" the surface. Secondly, it maintains the plant's state trajectory on this surface for all subsequent times. During the process, the control system's structure varies from one to another and thereby earning the name variable structure control. The control is

also called as the sliding mode control [56] to emphasize the importance of the sliding mode. Under sliding mode control, the system is designed to drive and then constrain the system state to lie within a neighborhood of the switching function. It's two main advantages are (1) the dynamic behaviour of the system may be tailored by the particular choice of switching function, and (2) the closed-loop response becomes totally insensitive to a particular class of uncertainty. Also, the ability to specify performance directly makes sliding mode control attractive from the design perspective. Trajectory of a system can be stabilized by a sliding mode controller. The system states 'slides' along the line *s=0* after the initial reaching phase. The particular $s = 0$ surface is chosen because it has desirable reduced-order dynamics when constrained to it. In this case, the $s = cx_1 + \dot{x}_1$, $c > 0$ surface corresponds to the first-order LTI system $\dot{x}_1 = -cx_1$, which has an exponentially stable origin. Now, we consider a simple example of the sliding mode controller design as under.

$$J\ddot{\theta}(t) = u(t) \tag{3.1}$$

where J is the inertia moment, $\ddot{\theta}(t)$ is the angle signal, and $u(t)$ is the control input. Firstly, we design the sliding mode function as

$$s(t) = ce(t) + \dot{e}(t) \tag{3.2}$$

where c must satisfy the Hurwitz condition, c> 0.
The tracking error and its derivative value are

$$e(t) = \theta(t) - \theta_d(t) \tag{3.3}$$

$$\dot{e}(t) = \dot{\theta}(t) - \dot{\theta_d}(t) \tag{3.4}$$

where $\theta(t)$ is the practical position signal, and $\theta_d(t)$ is the ideal position signal. Therefore, we have

$$\dot{s}(t) = c\dot{e}(t) + \ddot{e}(t) \tag{3.5}$$

$$\dot{s}(t) = c\dot{e}(t) + \ddot{\theta}(t) - \ddot{\theta_d}(t) \tag{3.6}$$

$$\dot{s}(t) = c\dot{e}(t) + \frac{1}{j}u - \ddot{\theta}(t) \tag{3.7}$$

and

$$s\dot{s} = s\left(c\dot{e} + \frac{1}{j}u - \ddot{\theta}_d\right) \tag{3.8}$$

Secondly, to satisfy the condition $s\dot{s}$, we design the sliding mode controller as

$$u(t) = J(-c\dot{e} + \ddot{\theta}_d - \eta\,sgn(s))$$ (3.9)

$$sgn(s) = \begin{cases} 1, & \text{if } s > 0 \\ 0, & \text{if } s = 0 \\ -1, & \text{if } s < 0 \end{cases}$$ (3.10)

Then, we get

$$s\dot{s} = -\eta\,|s| < 0$$ (3.11)

Sliding mode control is a nonlinear control method that alters the dynamics of a nonlinear system by the multiple control structures are designed so as to ensure that trajectories always move towards a switching condition. Therefore, the ultimate trajectory will not exist entirely within one control structure. The state-feedback control law is not a continuous function of time. Instead, it switches from one continuous structure to another based on the current position in the state space. Hence, sliding mode control is a variable structure control method. The multiple control structures are designed so as to ensure that trajectories always move towards a switching condition. Therefore, the ultimate trajectory will not exist entirely within one control structure. Instead, the ultimate trajectory will slide along the boundaries of the control structures. The motion of the system as it slides along these boundaries is called a sliding mode [57] and the geometrical locus consisting of the boundaries is called the sliding (hyper) surface. In the context of modern control theory, any variable structure system like a system under SMC, may be viewed as a special case of a hybrid dynamical system. Intuitively, sliding mode control uses practically infinite gain to force the trajectories of a dynamic system to slide along the restricted sliding mode subspace. Trajectories from this reduced-order sliding mode have desirable properties (e.g., the system naturally slides along it until it comes to rest at a desired equilibrium). The main strength of sliding mode control is its robustness. Because the control can be as simple as a switching between two states, it need not be precise and will not be sensitive to parameter variations that enter into the control channel. Additionally, because the control law is not a continuous function, the sliding mode can be reached in finite time (i.e., better than asymptotic behaviour). There are two steps in the SMC design. The first step is designing a sliding surface so that the plant restricted to the sliding surface has a desired system response. This means the state variables of the plant dynamics are constrained to satisfy another set of equations which define the so-called switching surface. The second step is constructing a switched feedback gains necessary to

drive the plant's state trajectory to the sliding surface. These constructions are built on the generalized Lyapunov stability theory.

3.2   Parameters of Sliding surface design

For linear system

$$\dot{x} = Ax + bu, x \in R^n, u \in R \tag{3.12}$$

where x is system state, A is an $n \times n$ matrix, b is an $n \times 1$ vector, and u is control input. A sliding variable can be designed as

$$s(x) = C^T x = \sum_{i=1}^{n} c_i x_i = \sum_{i=1}^{n-1} c_i x_i + x_n \tag{3.13}$$

where x is state vector, $c = [c_1 c_2 ... c_{n-1}]^T$.

In sliding mode control, parameters $c_1, c_2, ..., c_{n-1}$ should be selected so that the polynomial $p^{n-1} + c_{n-1} p^{n-2} + ... + c_2 p + c_1$ is a Hurwitz polynomial, where p is a Laplace operator.

For example, $n = 2$, $s(x) = c_1 x_1 + x_2$, to satisfy the condition that the polynomial $p + c_1 = 0$ should have a negative real part, i.e. $c > 0$.

Consider another example, $n = 3$, $s(x) = c_1 x_1 + c_2 x_2 + x_3$, to satisfy the condition that the polynomial $p^2 + c_2 p + c_1$ is Hurwitz, the eigenvalue of $p^2 + c_2 p + c_1 = 0$ should have a negative real part. For a positive constant λ in $(p + \lambda)^2 = 0$, we can get $p^2 + 2\lambda p + \lambda^2 = 0$. Therefore, we have $c_2 = 2\lambda$, $c_1 = \lambda^2$.

3.3   Sliding mode control based on Reaching law

Sliding mode based on reaching law includes reaching phase and sliding phase. The reaching phase drive system is to maintain a stable manifold and the sliding phase drive system ensures slide to equilibrium. The idea of sliding mode can be described in Fig. 3.1

3.3.1   Controller design

System Description

The plant is

$$\ddot{\theta} = -f(\theta, t) + bu(t) \tag{3.14}$$
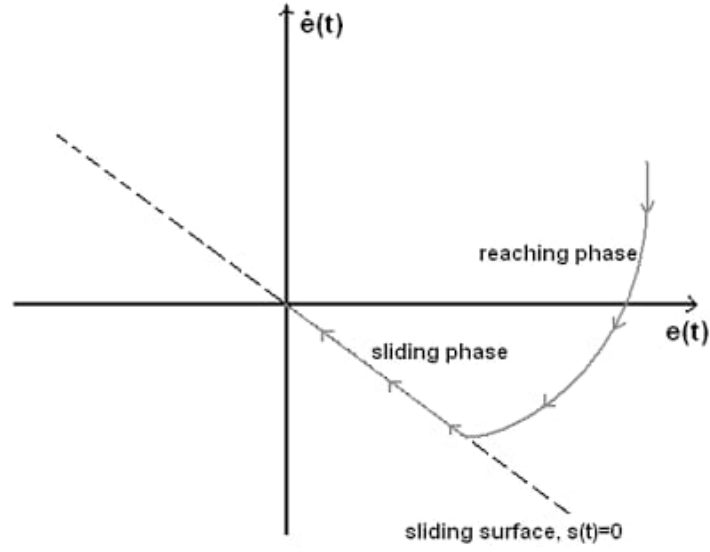
Fig. 3.1 The idea of sliding mode

where $f(\theta,t)$ and b are known and $b > 0$.

The sliding mode function is

$$s(t) = ce(t) + \dot{e}(t) \tag{3.15}$$

where c must satisfy Hurwitz condition $c > 0$.

The tracking error and its derivative value is

$$e(t) = r - \theta(t), \dot{e}(t) = \dot{r} - \dot{\theta}(t) \tag{3.16}$$

where r is the ideal position signal.

Therefore, we have

$$\dot{s}(t) = c\dot{e}(t) + \ddot{e}(t) = c(\dot{r} - \dot{\theta}(t)) + (\ddot{r} - \ddot{\theta}(t)) \tag{3.17}$$

$$\dot{s}(t) = c(\dot{r} - \dot{\theta}(t)) + \ddot{r} + f(\theta,t) - bu(t) - d(t) \tag{3.18}$$

According to the exponential reaching law, we have

$$\dot{s} = -\varepsilon sgn(s), \varepsilon > 0 \tag{3.19}$$

From Eqs. 3.17 and 3.19, we have

$$c(\dot{r} - \dot{\theta}(t)) + (\ddot{r} + f(\theta,t) - bu(t)) = -\varepsilon sgn(s) \tag{3.20}$$

Then we can get the sliding mode controller as

$$u(t) = \frac{1}{b}(\varepsilon sgn(s) + c(\dot{r} - \dot{\theta}(t)) + \ddot{r} + f(\theta,t)) \tag{3.21}$$

3.4   Robust Sliding mode control based on Reaching law

The purpose of this section is to explain SMC derivation.

3.4.1   System Description

The plant is

$$\ddot{\theta} = -f(\theta,t) + bu(t) + d(t) \tag{3.22}$$

where $f(\theta,t)$ and b are known and $b > 0$, $d(t)$ is the disturbance.
The sliding mode function is

$$s(t) = ce(t) + \dot{e}(t) \tag{3.23}$$

where c must satisfy Hurwitz condition $c > 0$.
The tracking error and its derivative value is

$$e(t) = r - \theta(t) \tag{3.24}$$

$$\dot{e}(t) = \dot{r} - \dot{\theta}(t) \tag{3.25}$$

where r is the ideal position signal.
Therefore, we have

$$\dot{s}(t) = c\dot{e}(t) + \ddot{e}(t) \tag{3.26}$$

$$\dot{s}(t) = c(\dot{r} - \dot{\theta}(t)) + (\ddot{r} - \ddot{\theta}(t)) \tag{3.27}$$

$$\dot{s}(t) = c(\dot{r} - \dot{\theta}(t)) + (\ddot{r} + f - bu - d) \tag{3.28}$$

Using the exponential reaching law, we have

$$\dot{s} = -\varepsilon sgn(s), \varepsilon > 0 \tag{3.29}$$

From Eqs.3.28 and 3.29, we have

$$c(\dot{r} - \dot{\theta}) + (\ddot{r} + f - bu - d) = -\varepsilon sgn(s) \tag{3.30}$$

If we design the sliding mode controller as

$$u(t) = \frac{1}{b}(\varepsilon sgn(s) + c(\dot{r} - \dot{\theta}) + \ddot{r} + f - d) \tag{3.31}$$

Obviously, all quantities on the right-hand side of Eq. 3.30 are known except the disturbance d, which is unknown. Thus the control law Eq. 3.30 is incomplete. To solve this problem, d in Eq. 3.30 is replaced by a conservative known quantity d_c. Then we can get the sliding mode controller as

$$u(t) = \frac{1}{b}(\varepsilon sgn(s) + c(\dot{r} - \dot{\theta}) + \ddot{r} + f - d_c)) \tag{3.32}$$

where, d_c is chosen to guarantee the reaching condition. Substituting Eq. 3.32 into Eq. 3.28 and simplifying the result, we get

$$\dot{s}(t) = -\varepsilon sgn(s) + d_c - d \tag{3.33}$$

The term d_c can be chosen to ensure the reaching condition. It is reasonable to assume that d is bounded, therefore, so is d_c. That is

$$d_L \leq d(t) \leq d_U \tag{3.34}$$

where the bounds d_L and d_U are known. Referring to Eq. 3.33, d_c is chosen according to the following logic;
When $s(t) > 0$, $\dot{s}(t) = -\varepsilon + d_c - d$, we want $\dot{s}(t) < 0$, so let $d_c = d_L$
When $s(t) < 0$, $\dot{s}(t) = \varepsilon + d_c - d$, we want $\dot{s}(t) > 0$, so let $d_c = d_U$
Therefore, if we define $d_1 = \frac{d_U - d_L}{2}$, $d_1 = \frac{d_U + d_L}{2}$, then we can get

$$d_c = d_2 - d_1 sgn(s) \tag{3.35}$$

3.4.2   Simulation Example

Consider the plant as

$$\ddot{\theta}(t) = -f(\theta, t) + bu(t) + d(t) \tag{3.36}$$

where $\ddot{\theta}(t) = -25\dot{\theta}$, $b = 133$, $d(t) = 10sin(\Pi t)$, the intial state is set as [-0.15 -0.15], using controller Eq. 3.32, $c = 15, \varepsilon = 0.5, k = 10$, the results can be seen in Figs. 3.2 - 3.5.
Fig. 3.2 depicts the position tracking performance of SMC for a second order system expressed in Eq. 3.36. The disturbance imposed upon the system was nullified by the SMC and closed loop system response stabilized in minimum amount of time. Fig. 3.3 and Fig. 3.4 depicts the sliding surface and control input of the controller. High frequency oscillations

known as chattering can be clearly observed due to discontinuous switching function signum. Phase trajectory of SMC for second order system are shown in Fig. 3.5.
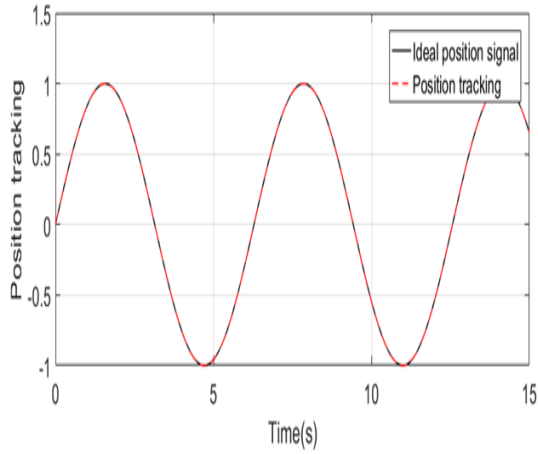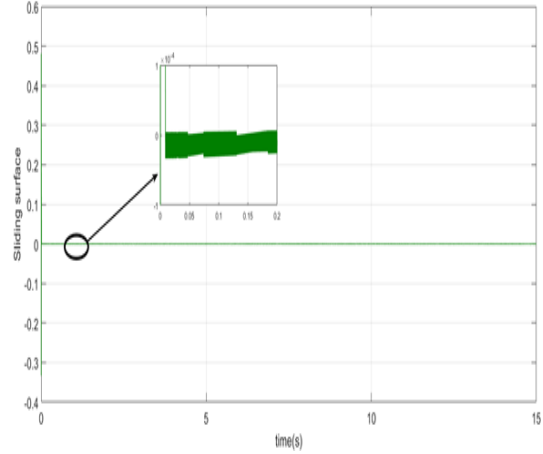

Fig. 3.2 SMC ideal position tracking
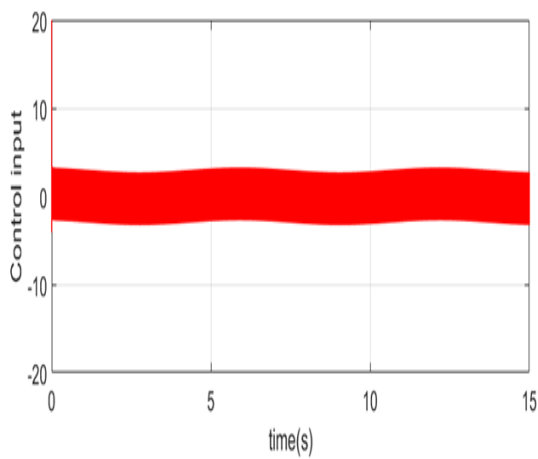

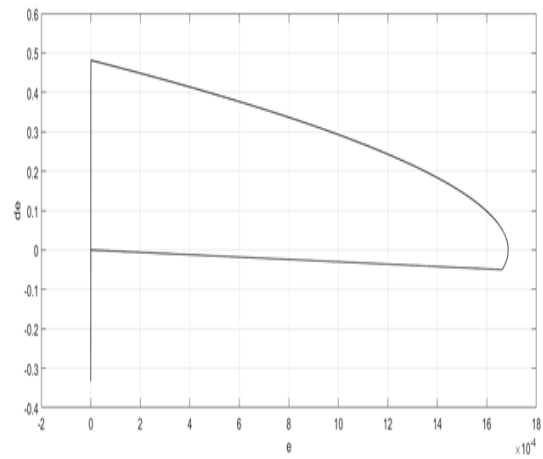Fig. 3.3 Sliding surface

Fig. 3.4 Control input

Fig. 3.5 Phase trajectory

3.5　Adaptive sliding mode controller design

The Sliding Mode Control is a very popular strategy for control of nonlinear uncertain systems, with a very large frame of applications fields [58, 59]. Due to the use of the discontinuous function, its main features are

- the robustness of closed-loop system

- and the finite-time convergence.

However, its design requires the knowledge of the bound on the uncertainties, which could be, from a practical point of view, a hard task: it often follows that this bound is overestimated, which yields excessive gain. Then, the main drawback of the sliding mode control, the well-known chattering phenomenon is important and could damage actuators and systems. A first way to reduce the chattering is the use of a boundary layer: in this case, many approaches have proposed adequate controller gains tuning [60]. A second way to decrease the effect of the chattering phenomenon is the use of higher order sliding mode controller [61, 62]. However, in both these control approaches, knowledge of the bound on the uncertainties is required. As the objective is the non-requirement of the uncertainties is required. As the objective is the non-requirement of the uncertainties bound, another way consists in using adaptive sliding mode, the goal being to ensure a dynamic adaptation of the control gain to be as small as possible whereas sufficient to counteract the uncertainties and perturbations.

The basic idea of the Adaptive Control Approach consists in designing the systems exhibiting the same dynamics properties under uncertainty conditions based on utilization of current information. It involves modifying the control law used by a controller to cope with the fact that the parameters of the system being controlled are slowly time-varying or uncertain. Even more, adaptive control implies improving dynamic characteristics while properties of a controlled plant or environment are varying [63]. Without adaptation the original SMC demonstrates robustness properties with respect to parameter variations and disturbances [64]. The first attempts to apply the ideas of adaptation in SMC were made in the 60's [65]: the control efficiency was improved by changing the position or equation of the discontinuity surfaces without any information on a plant parameters. The design idea might be formulated as follows: if sliding mode exists, then the coefficients of switching plane can be varied to improve the system dynamics. However those early publications did not take into account the main obstacle for SMC application- the chattering phenomenon which is inherent in sliding motions. This phenomenon is well-known from literature on power converters and referred to as 'ripple' [66]. Then the efforts of the researchers were oriented to the application

of adaptability principles to reduce the effect of chattering. Since the amplitude of chattering is proportional to discontinuity magnitude in control, one of possible adaptation methods is related to reducing this magnitude to the minimum admissible value dictated by the conditions for SM to exist. So, in [67] the control gain depended on the distance of system state to a discontinuity surface. The tracks of adaptability can be found in the first publications about variable structure systems with SM with the control gain proportional the system state. This problem is an exciting challenge for applications given that, in many cases, gains are also overestimated, which gives larger control magnitude and larger chattering. In order to adapt the gain, many controllers based on fuzzy tools [59] have been published; however, these papers do not guarantee the tracking performances. In [68] gain dynamics directly depends on the tracking error (sliding variable): the control gain is increasing since sliding mode is not established. Once this is the case, gain dynamics equals zero. The main drawback of this approach is the gain over-estimation with respect to uncertainties bound. Furthermore, this approach is not directly applicable, but requires modifications for its application to real systems: thus, the sign function is replaced by a saturation function where the boundary layer width affects accuracy and robustness. Furthermore, no boundary layer width tuning methodology is provided. A method proposed in [69] in order to limit the switching gain must be mentioned. The idea is based on use of equivalent control: once sliding mode occurs, disturbance magnitude is evaluable and allows an adequate tuning of control gain. However, this approach requires the knowledge of uncertainties/perturbations bounds and the use of low-pass filter, which introduces signal magnitude attenuation, delay and transient behavior when disturbances are acting. In [70] a gain-adaptation algorithm is proposed by using sliding mode disturbance observer. The main drawback is that the knowledge of uncertainties bounds is required to design observer-based controller. There exist also adaptive SMC (ASMC) algorithms that allow adjusting dynamically the control gains without knowledge of uncertainties/perturbations bounds. In particular, several adaptive fuzzy SMC algorithms were proposed. However, they do not guarantee the tracking performance or overestimate the switching control gains as in [68]. Of course, another efficient tool to suppress chattering is the application of state observers [71], but for this method the plant parameters are assumed to be known.

Now we give adaptive sliding mode controller example as follows.

3.5.1   Controller Design

Consider the plant as

$$\ddot{\theta} = -f(\theta, t) + bu + d \tag{3.37}$$

where $-f(\theta,t) = 25$, $b = 133$, $d = 10sin(\Pi t)$

Let the desired output be θ_d, and denote

$$e = \theta - \theta_d \tag{3.38}$$

Define the sliding mode function as

$$s = ce + \dot{e}, c > 0 \tag{3.39}$$

then

$$s = ce + (\dot{\theta} - \dot{\theta}_d) = \dot{\theta} - (\dot{\theta}_d - ce) = \dot{\theta} - q \tag{3.40}$$

Therefore,

$$\dot{s} = \ddot{\theta} - \dot{q} \tag{3.41}$$

and $q = \dot{\theta}_d - ce$.

Substitute Eq.3.37 in above Eq. 3.41

$$\dot{s} = -f(\theta,t) + bu + d - \dot{q} \tag{3.42}$$

The controller is selected as,

$$u = u_a + u_s \tag{3.43}$$

where

$$u_s = -ksgn(s) \tag{3.44}$$

Now for u_a, Eq. 3.42 can be written as

$$0 = -f(\theta,t) + bu_a + d - \dot{q} \tag{3.45}$$

$$u_a = \frac{1}{b}(f(\theta,t) + \dot{q} - \hat{d}) \tag{3.46}$$

Select the Lyaunov function as

$$V = \frac{1}{2}s^2 + \frac{1}{2\gamma}\tilde{d}^2 \tag{3.47}$$

where $\tilde{d} = \hat{d} - d, \gamma > 0$

We then get

$$\dot{V} = s(\dot{s}) + \frac{1}{\gamma}\tilde{d}\dot{\hat{d}} \tag{3.48}$$

$\dot{s}$ from Eq. 3.42

$$\dot{V} = s(-f(\theta,t) + bu + d - \dot{q}) + \frac{1}{\gamma}\tilde{d}\dot{\hat{d}} \tag{3.49}$$

From Eq. 3.43,

$$\dot{V} = s(-f(\theta,t) + b(u_a + u_s) + d - \dot{q}) + \frac{1}{\gamma}\tilde{d}\dot{\hat{d}} \tag{3.50}$$

It becomes,

$$\dot{V} = s(-f(\theta,t) + b(\frac{1}{b}(f(\theta,t) + \dot{q} - \hat{d}) - ksgn(s)) + d - \dot{q}) + \frac{1}{\gamma}\tilde{d}\dot{\hat{d}} \tag{3.51}$$

After simplification,

$$\dot{V} = s(d - \hat{d} - ksgn(s)) + \frac{1}{\gamma}\tilde{d}\dot{\hat{d}} \tag{3.52}$$

$$\dot{V} = s(\tilde{d} - ksgn(s)) + \frac{1}{\gamma}\tilde{d}\dot{\hat{d}} \tag{3.53}$$

$$\dot{V} = s\tilde{d} - k|s| + \frac{1}{\gamma}\tilde{d}\dot{\hat{d}} \tag{3.54}$$

Design the adaptive law as

$$\dot{\hat{d}} = -\gamma s \tag{3.55}$$

$$\dot{V} = s\tilde{d} - k|s| - s\tilde{d} \tag{3.56}$$

It can be proved that $\dot{V} \leq 0$ when the switching gain $k > 0$ and closed loop system is stable.

$$\dot{V} = -k|s| \tag{3.57}$$

The simulation results are shown in Figs. 3.6 - 3.9. Fig. 3.6 depicts the performance of Adaptive SMC for a second order system. It is clear from the figure that the closed loop response of system is stable and output of system tracks the reference signal in the presence of external disturbance with negligible error. Performance vise it can be observed from both Fig. 3.2 and Fig. 3.6 that both controllers i.e. SMC and Adpative SMC show robust behaviour in nullifying the external disturbances. Major difference between SMC and Adaptive SMC can be observed after comparing the sliding surfaces and control inputs comparison of both controllers for same system with same environmental conditions as shown in Figs. 3.3 & 3.4 for SMC and Figs. 3.7 & 3.8 for Adaptive SMC. The adaptive law derived in Eq. 3.55 adapts the disturbances on the systems and subtracts the overall effect of disturbance thereby reducing the chattering effect of discontinuous switching function signum.

From Figs. 3.7 & 3.8 it is clear that Adaptive SMC offers far less amount of chattering as

compared to classical SMC and therefore it's more feasible for implementation on hardware in comparison with classical SMC. Figs. 3.9 & 3.10 depicts the phase trajectory and adaptive law uncertainty estimation of Adaptive SMC. As mentioned in the previous section that disturbance imposed upon the system was $d(t) = 10sin(\Pi t)$. Adaptive law derived in Eq. 3.55 was able to successfully estimate the disturbance applied to the system.
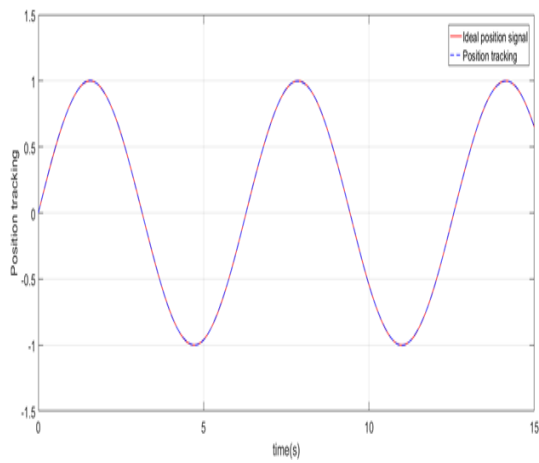
Fig. 3.6 Adaptive SMC ideal position tracking   Fig. 3.7 Adaptive SMC Sliding surface
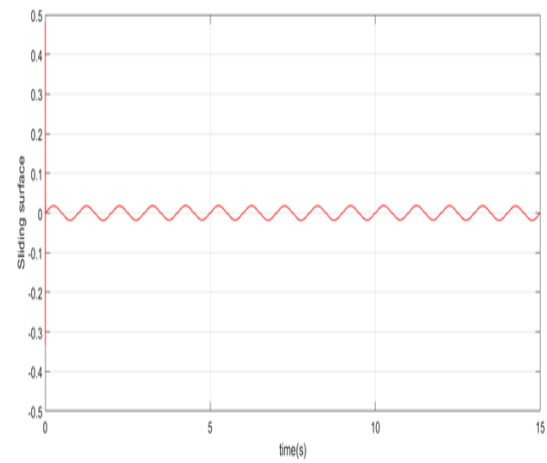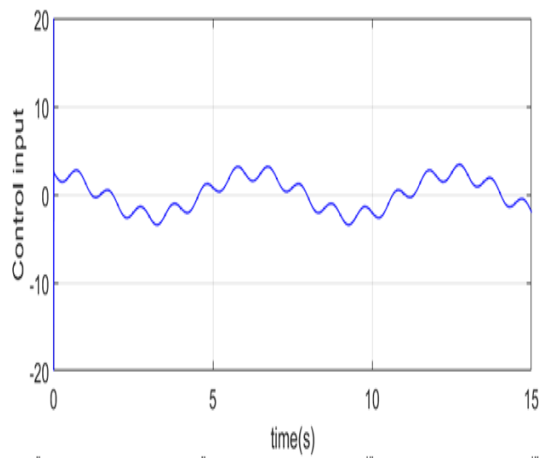

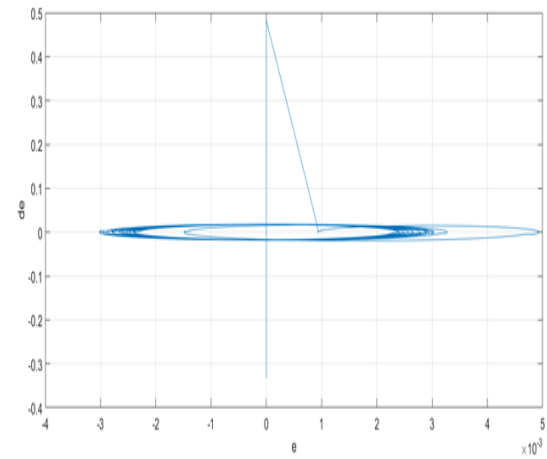Fig. 3.8 Adaptive Control input   Fig. 3.9 Adaptive Phase trajectory
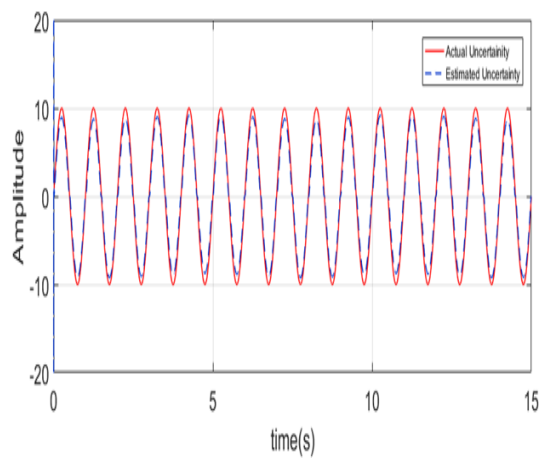

Fig. 3.10 Adaptive Uncertainty Estimation

Part II

Contribution of SMC and Adaptive SMC in MPPT problem

Chapter 4

SMC and Adaptive SMC Control schemes for Maximum Power Point Tracking of Photovoltaic Systems

This chapter presents sliding mode control which is widely used for increasing the output power of photovoltaic sources. These sliding-mode controllers are primarily based on one-loop or two-loop schemes. The two-loop scheme is composed of two loops, i.e., searching and tracking loops. A maximum power point searching unit is utilized in the searching loop, and a tracking controller is utilized in the other loop to extract the maximum photovoltaic power. Compared to this scheme, the one-loop scheme can extract the maximum photovoltaic power without any searching algorithm. In this study, dynamic equations of a typical photovoltaic power source are derived using the state-space averaging method. Afterwards, two-loop sliding mode control and adaptive sliding mode control schemes are derived for extracting the maximum power. Stability of the control law is guaranteed using Lyapunov theory. P&O, PSO and IPSM MPPT algorithms are used for maximum power point searching in the two-loop scheme.

4.1 Introduction

Maximum power point (MPP) tracking units should be utilized in photovoltaic sources to increase their efficiency. Fig. 4.1 shows that DC converters are usually utilized between the load and PV cells for MPP tracking. However, a tracking controller is required to control this converter. In this case, many MPP tracking controllers have been introduced, e.g., PID controller [72, 73], passivity-based control [74], input-output linearization [75], feedback

linearization [76] and sliding-mode control (SMC) [77, 78]. Among these controllers, SMC is more popular due to its global stability and robustness. However, the primary problem of the SMC is its chattering problem. The discontinuous nature of the control law usually leads to the chattering problem. Chattering deteriorates the performance of the control systems [79]. SMC is a type of variable structure controller [79]. Each SMC is composed
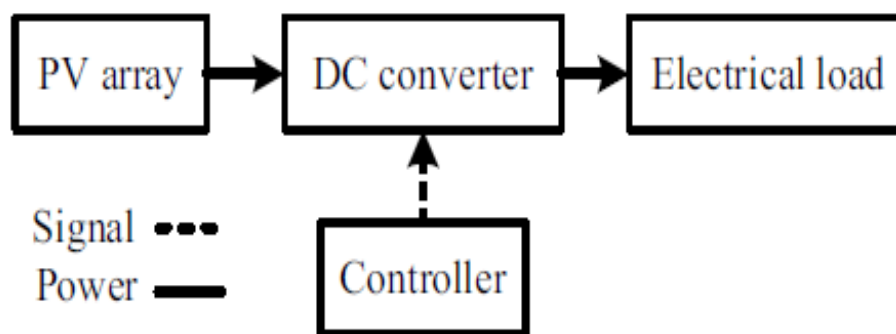

Fig. 4.1 A typical photovoltaic power source

of a switching surface and a control law. One-loop and two-loop SMCs are shown in Fig. 4.2. In the one-loop scheme, the MPP tracking controller does not require MPP On the other hand, the two-loop scheme requires an additional algorithm for MPP searching. The one-loop SMC was introduced in [77]. In this scheme, the switching surface is selected as dP/dI [77] or dP/dV [80], where P, I and V are power, current and voltage, respectively. By converging the switching surface to zero, the maximum power will be extracted. The number of required voltage sensors for this scheme is decreased in [49]. The one-loop control scheme can also be used for grid-connected PV systems [81]. In two-loop scheme, the first and second loops are used for MPP searching and MPP tracking, respectively. The interaction between the loops must be considered in the designing procedure, i.e., the tracking loop should be faster than the searching loop. In this context, a terminal SMC was introduced in [82], which ensures the finite time stability. Thus, it can be shown that the tracking loop is always faster than the searching loop. In this thesis, two-loop control scheme is chosen. In the first loop of searching to calculate the MPP an IPSM optimization algorithm is used to generate the reference voltage for the MPP tracking loop i.e. the controller loop. Two other optimization algorithms, namely, P&O and PSO along with IPSM MPPT has been conducted for the proposed system. In the second tracking loop for the controller part, first an integer order SMC controller formulation is developed based on the nonlinear mathematical model of PV panel with a boost converter. Classical SMC generally suffer from the problem of
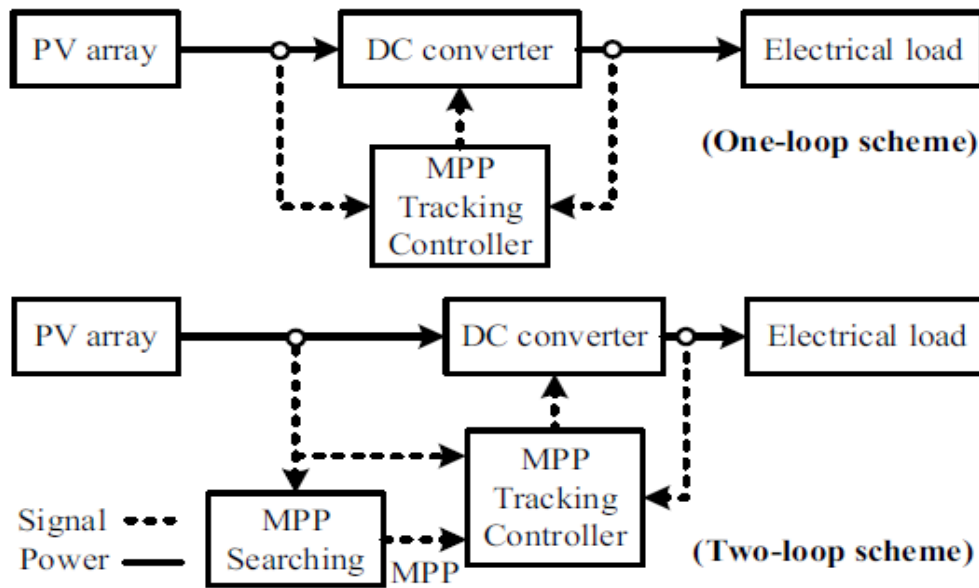
Fig. 4.2 One-loop and two-loop control schemes

'Chattering', which is a very high frequency oscillation of the sliding variable around the sliding manifold. Therefore, authors have introduced Adaptive version of SMC also in this study which reduce chattering phenomenon and limits high frequency oscillations present in classical SMC.

4.2 SMC Controller Design

The proposed scheme implemented in this work is presented in Fig. 4.3. Stand-alone PV system is used which consists of a PV panel, DC-DC boost converter, a load and a control loop that produces PWM signal to the step-up converter for MPPT process. In this implementation, the voltage and current of the PV array are provided to the optimization algorithm employing P&O which defines the reference to the SMC controller to provide reference peak power voltage, which can be tracked by the proposed non-linear controller. The controller has been derived using the mathematical model of a non- inverting boost converter and generates an output signal , which controls the duty ratio of the PWM signal provided to the converter switches. The MPPT-based P&O generates the reference voltage V_{ref} , which is compared with panel voltage V_{PV} to generate an error signal, which is supplied to the improved sliding mode controller. The controller generates the control input μ , which controls the PWM signal width and drives the converter to track the reference voltage. Hence, operating the

PV module on this reference voltage will ensure that maximum power is generated by the
system.
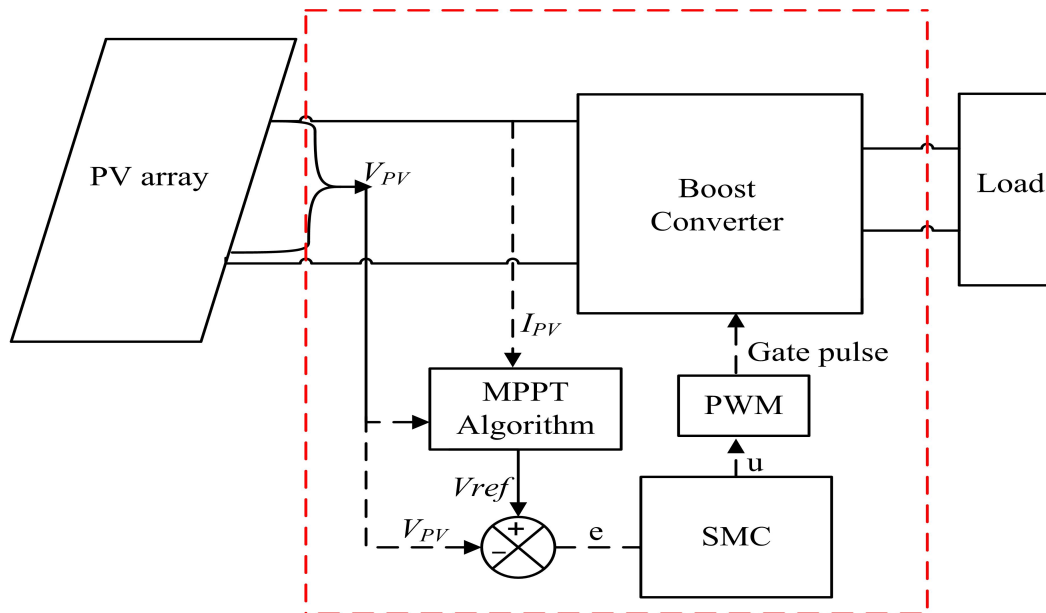
Fig. 4.3 System scheme based on sliding mode controller (SMC).

4.2.1   PV Model

Mathematical models are used to describe the operation and behavior of the PV panels
in the calculation of the current-voltage characteristic. The current voltage (I-V relation)
mathematical equation of the solar cell is implicit and non-linear. For precise PV cell
modeling and better accuracy, in this work, we use a two diode PV model which involves
identification of more parameters at the expense of longer computational time and is known
as being a seven-parameter model [83]. Simulations are based on the double-diode model,
since their estimation is more useful with other models (i.e., single diode model) [84]. The
PV panel based on the two diode model is shown in Fig. 4.4. To operate the PV panel at
MPP, a DC-DC converter controlled by the MPPT is inserted between the PV panel and
the load. DC-DC converters are used widely for the efficient management of energy in PV
systems. The boost converter has been chosen for this work [85], as shown in Fig. 4.4.
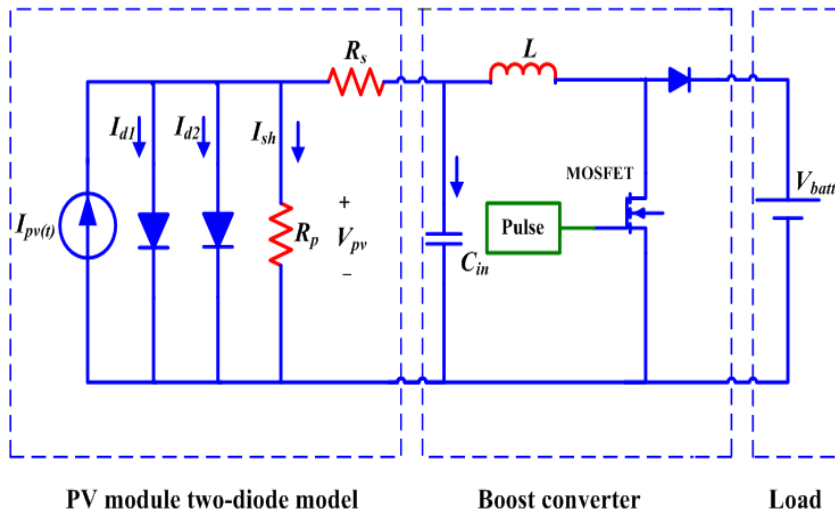
Fig. 4.4 Circuit diagram of the two-diode model PV system.

4.2.2 MPPT Algorithms

MPPT algorithms are used to generate the reference voltage V_{ref} of the peak power panel voltage to extract maximum power from the PV array under varying environmental conditions. The description of the MPPT algorithms is discussed in this section which are implemented in this study.

a). MPPT algorithm based on P&O

The P&O MPPT algorithm is based on managing either the voltage command or the boost converter input current. Subsequently, the measure of power converted from the panel is estimated. The P&O algorithm adopted methodology description is explained in [86], in which an integer order sliding mode controller had been proposed for the two-diode model-based PV system. P&O MPPT algorithm had been used in [87] in order to be able to extract the maximum power from the panel and providing the reference voltage to the sliding mode controller acting as a voltage loop controller. Here, the controller is modified by Adaptive SMC [88] to address the chattering phenomenon which was present in [87]. The P&O algorithm flow diagram is shown in Fig. 4.5 which is executed in PSIM simulation tools.
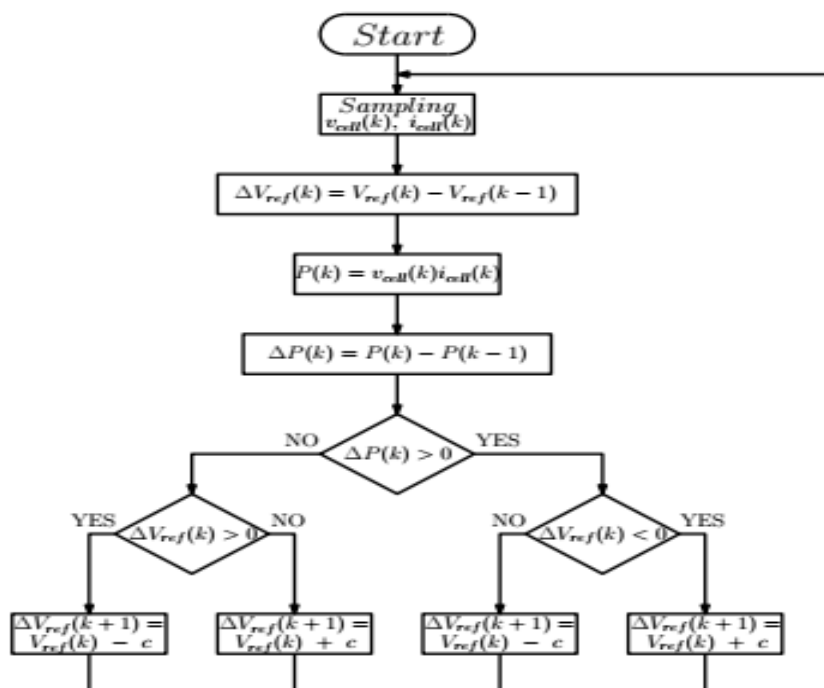
Fig. 4.5 Perturb and Observe algorithm (P&O).

b). MPPT algorithm based on PSO

Particles Swarm Optimization (PSO) [36], algorithms are strategies based on a heuristic search that use a population, characterized with stochastic features, which are motivated by swarms. Each one of such particles, constitutes a candidate solution. PSO calculations produce new particles positions and features on the basis of its interaction with the rest. For example, for what matters to the particle position, it is determined on the basis of particles in a superior situation. This superior situation, in our case study, corresponds to a reference voltage that generate a better, superior, power conversion. As an iteration-based approach, once a particle with superior characteristics is found, the rest of the particles will be affected by this. This wining particle will constitute he output of the algorithm. Flow diagram of the PSO algorithm is depicted in Fig. 4.6.
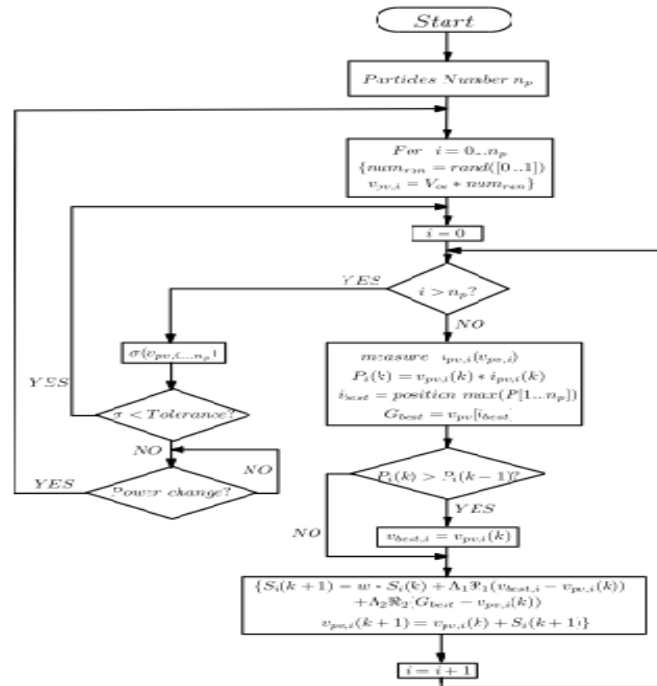
Fig. 4.6 Particle Swarm Optimization algorithm (PSO).

c). MPPT algorithm based on IPSM

In this case, IPSM is an improvement with respect to the Pattern Search Method (PSM) from [89]. Pattern Search algorithms are defined along two main constitutive parts: first, an arrangement of mesh definitions and, second a list of polling conditions. Every component of the mesh is a solution candidate. Pattern search are also iterative methods. Therefore, at each iteration, the meshes move towards the best position, according to a convergence condition. In this case, the search is actualized with respect to the one in [26] by introducing, also, search at adjoining members to the one that is defined as with the best position. This update, for the case at hand, introduces the possibility to guarantee appropriate convergence even in cases of radiation or partial shading.The algorithm applied to the power conversion of a photovoltaic panel is portrayed in Fig. 4.7.
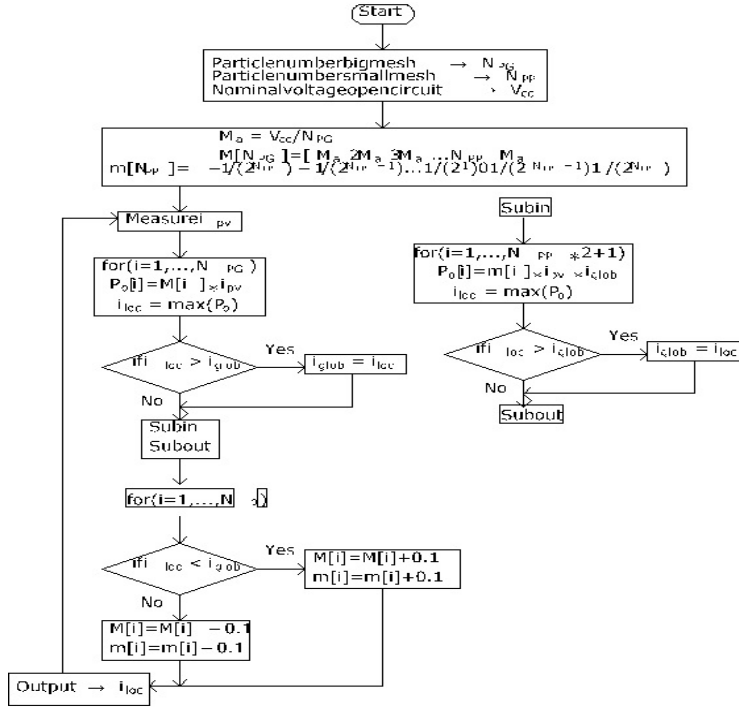
Fig. 4.7 Improved Pattern Search algorithm (IPSM).

4.2.3   Control Scheme

A. DC-DC Converter Model

Power electronic converters (DC-DC) are used in photovoltaic systems as an adaptation stage
between the PV panel and the load. The DC-DC power converter is connected to adjust the
PV panel output voltage to maximize the solar power generation. In this work, we adapt a
boost converter which steps up voltage from its input (PV array) to its output (load), in order
to operate the PV panel at the MPP. It is assumed that the converter is operating in continuous
conduction mode. The converter is used to regulate the PV module output voltage, V_{PV} , in
order to extract as much power as possible from the PV module. Referring to Fig. 4.8, the
dynamics of the boost converter is given by [90]:

$$I_{cin} = C_{in}\frac{dV_{pv}}{dt} = I_{pv} - I_L \tag{4.1}$$

$$V_L = L\frac{dL}{dt} = V_{PV} - V_b(1-u) \tag{4.2}$$

where I_{cin}, I_{PV}, V_p, C_{cin}, V_L, I_L, and L represent capacitor current, PV current, battery
voltage, input capacitor capacitance, voltage across inductor, inductor current, and inductor

PV Panel
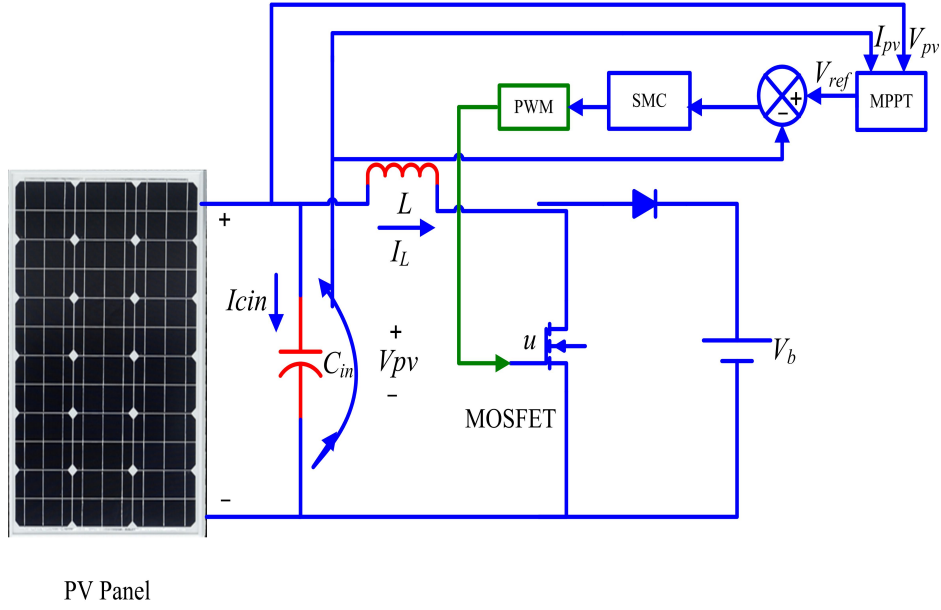
Fig. 4.8 Circuit diagram of the proposed control scheme.

inductance, respectively. Re arranging Eq. (4.1&4.2) we have:

$$\frac{dV_{pv}}{dt} = \frac{-I_L}{C_{in}} + \frac{I_{pv}}{C_{in}} \tag{4.3}$$

$$\frac{dL}{dt} = \frac{V_{PV}}{L} - \frac{V_b}{L} + \frac{u}{L} \tag{4.4}$$

Eq. (4.3&4.4) can be written in state space form as

$$\begin{bmatrix} \dot{V_{PV}} \\ \dot{I_L} \end{bmatrix} = \begin{bmatrix} 0 & -\frac{1}{C_{in}} \\ \frac{1}{L} & 0 \end{bmatrix} \begin{bmatrix} \dot{V_{PV}} \\ \dot{I_L} \end{bmatrix} \tag{4.5}$$

$$+ \begin{bmatrix} \frac{I_{PV}}{C_{in}} & 0 \\ \frac{-V_b}{L} & 0 \end{bmatrix} \begin{bmatrix} 1 \\ 0 \end{bmatrix} + \begin{bmatrix} 0 \\ \frac{-V_b}{L} \end{bmatrix} \tag{4.6}$$

Eq. 4.6 can be re-written in generalized form as

$$\dot{X} = f(X,t) + J(X,t) + h(X,t)u \tag{4.7}$$

Here $X = [x_1 \quad x_2]^T = [V_{PV} \quad I_L]^T$ represents PV panel voltage and inductor current $J = (X,t)$ and $h = (X,t)$ represents nominal system inputs and u represents the control excitation. I_{PV}, V_b, C_{in}, L represents PV current, bulk voltage, input capacitor capacitance and Inductor

inductance respectively.

$$f(X,t) = \begin{pmatrix} 0 & -\frac{1}{C_{in}} \\ \frac{1}{L} & 0 \end{pmatrix} \tag{4.8}$$

$$J(X,t) = \begin{bmatrix} \frac{I_{PV}}{C_{in}} & 0 \\ \frac{-V_b}{L} & 0 \end{bmatrix} \tag{4.9}$$

$$h(X,t) = \begin{pmatrix} 0 \\ V_b/L \end{pmatrix} \tag{4.10}$$

B. Controller Formulation

The objective of the closed loop control system is that panel voltage, V_{PV}, must strictly follow the V_{PV-ref} generated by the MPPT algorithm so that maximum power can be extracted from the PV panel under varying sunlight and temperature. The reference signal generated by the MPPT algorithm can be written as:

$$X_d = [x_d \ \dot{x}_d] = [V_{PV-ref} \ \dot{V_{PV-ref}}] \tag{4.11}$$

The tracking error can be defined as

$$\begin{cases} e_1 & = & x_1 - x_d \\ e_2 & = & \dot{e}_1 \\ e_2 & = & x_2 - \dot{x}_d \\ \dot{e}_2 & = & \dot{x}_2 - \ddot{x}_d \end{cases} \tag{4.12}$$

Sliding surface is chosen as

$$s = c_1 e_1 + e_2 \tag{4.13}$$

Here $c_1 > 0$ is the design parameter. Differentiating Eq. 4.13 on both sides

$$\dot{s} = c_1 e_2 + \dot{e}_2 \tag{4.14}$$

By combining Eq. 4.7 and Eq. 4.14 one can obtain

$$\dot{s} = c_1 e_2 + f(X,t) + J(X,t) + h(X,t)u - \ddot{x}_d \tag{4.15}$$

To derive the control set $\dot{s} = 0$, the desired response can be achieved by choosing the control law as

$$\begin{pmatrix} u = & u_{eq} + u_s \\ u_{eq} = & h(X,t)^{-1}[\ddot{x}_d - f(X,t) - J(X,t) - c_1 e_2] \\ u_s = & -h(X,t)^{-1} k_s sgn(s) \end{pmatrix} \tag{4.16}$$

Where u_{eq} is the equivalent control item to drive the nominal part of system, u_s is the robust switching control item. $sgn(.)$ is the signum function defined as:

$$sgn(s) = \begin{cases} +1 & if s > 0 \\ 0 & if s = 0 \\ -1 & if s < 0 \end{cases} \tag{4.17}$$

C. Stability Proof of the Proposed Controller

The stability of the proposed control scheme can be proved by choosing the Lyapunov candidate function as:

$$V = \frac{1}{2}s^2 \tag{4.18}$$

where s represents the sliding surface chosen in Eq. 4.38. According to Lyapunov, the control system will be stable if the derivative of the Lyapunov candidate is negative along the closed-loop system trajectories. Thus, by taking the derivative of Eq 4.18, we get:

$$\dot{V} = s\dot{s} \tag{4.19}$$

Putting $\dot{s}$ from Eq. 4.15 into Eq. 4.19, we get:

$$\dot{V} = s(c_1 e_2 + f(X,t) + J(X,t) + h(X,t)u - \ddot{x}_d) \tag{4.20}$$

Putting the value of 'u' from Eq. 4.16 into Eq 4.20 and simplifying, we obtain:

$$\dot{V} = s(-k_s sgn(s)) \leq (-k_s |s|) \leq 0 \tag{4.21}$$

It can be shown that $\dot{V} \leq 0$ if the switching gain $k_s > 0$ and the closed loop system is stable.

4.3 Adaptive Sliding Mode Controller Design

The design of adaptive SMC controller is discussed for the proposed PV system. In order to effectively track the reference voltage generated by MPPT algorithms (P&O, PSO and IPSM)

and to extract maximum power from the PV array, adaptive SMC controller is developed in this section.

4.3.1 Control law

Fig. 4.9 shows schematic circuital representation of the proposed adaptive SMC controller for the proposed PV system. The operation of the work has been described in detail in Sect.4.2. Therefore, the dynamics of the DC-DC boost converter is given by:
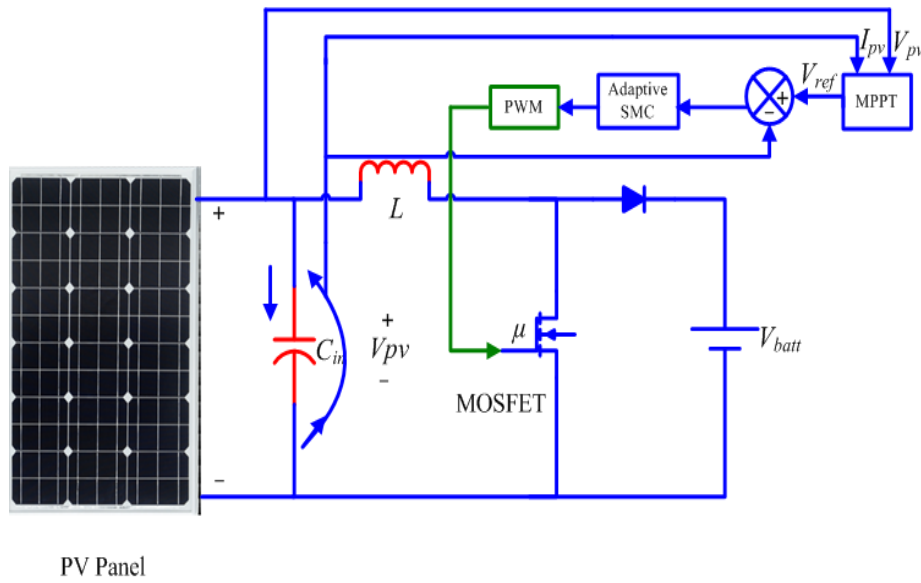

Fig. 4.9 System scheme based on Adaptive SMC control.

$$I_{cin} = (C_{in} + \Delta C_{in})\frac{dV_{pv}}{dt} = I_{pv} - I_L \tag{4.22}$$

$$V_L = (L + \Delta L)\frac{dI_L}{dt} = V_{pv} - V_b(1 - u) \tag{4.23}$$

I_{cin}, I_{pv}, V_b, C_{in}, and L represents nominal values of capacitor current, PV current, battery voltage, input capacitor capacitance, voltage across inductor, inductor current and Inductor inductance, respectively Δ is the uncertainty term which is introduced to add uncertainties in the system parameters under climatic changes. Re arranging Eq. (4.22) and Eq. (4.23) we have

$$\dot{V}_{pv} = -\frac{I_L}{C_{in} + \Delta C_{in}} + \frac{I_{pv}}{C_{in} + \Delta C_{in}} \tag{4.24}$$

$$\dot{I}_L = \frac{V_{pv}}{L + \Delta L} - \frac{V_b}{L + \Delta L} + \frac{V_b}{L + \Delta L}u \tag{4.25}$$

In state space form Eq. (4.24&4.25) can be written form as

$$
\begin{bmatrix} \dot{V}_{pv} \\ \dot{I}_L \end{bmatrix} = \begin{bmatrix} 0 & -\frac{1}{C_{in}+\Delta C_{in}} \\ \frac{1}{L+\Delta L} & 0 \end{bmatrix} \begin{bmatrix} V_{pv} \\ I_L \end{bmatrix} + \begin{bmatrix} \frac{I_{pv}}{C_{in}+\Delta C_{in}} & 0 \\ \frac{-V_b}{L+\Delta L} & 0 \end{bmatrix} \begin{bmatrix} 1 \\ 0 \end{bmatrix} + \begin{bmatrix} 0 \\ \frac{V_b}{L+\Delta L} \end{bmatrix} u
$$

(4.26)

The generalized form of Eq. 4.26 can be re-written as

$$
\dot{X} = f(X,t) + J(X,t) + h(X,t)u + \Delta f(X,t) + \Delta J(X,t) + \Delta h(X,t)u + d(X,t) \quad (4.27)
$$

Here $X = [x_1 \quad x_2]^T = [V_{pv} \quad I_L]^T$ represents PV panel voltage and inductor current $f = (X,t)$, $J = (X,t)$ and $h = (X,t)$ represents nominal system inputs and u represents the control excitation. $\Delta f = (X,t)$, $\Delta J = (X,t)$ and $\Delta, h = (X,t)$ represents the uncertainties terms and $d(X,t)$ represents unknown disturbances.

$$
f(X,t) = \begin{bmatrix} 0 & -\frac{1}{C_{in}} \\ \frac{1}{L} & 0 \end{bmatrix}
$$

(4.28)

$$
J(X,t) = \begin{bmatrix} \frac{I_{PV}}{C_{in}} & 0 \\ \frac{-V_b}{L} & 0 \end{bmatrix}
$$

(4.29)

$$
h(X,t) = \begin{bmatrix} 0 \\ \frac{V_b}{L} \end{bmatrix}
$$

(4.30)

$$
\Delta f(X,t) = \begin{bmatrix} 0 & \frac{-1}{\Delta C_{in}} \\ \frac{1}{\Delta L} & 0 \end{bmatrix}
$$

(4.31)

$$
\Delta J(X,t) = \begin{bmatrix} \frac{I_{PV}}{\Delta C_{in}} & 0 \\ \frac{-V_b}{\Delta L} & 0 \end{bmatrix}
$$

(4.32)

$$
\Delta h(X,t) = \begin{bmatrix} 0 \\ \frac{V_b}{\Delta L} \end{bmatrix}
$$

(4.33)

Eq. 4.27 can be further generalized as

$$
\dot{X} = f(X,t) + J(X,t) + h(X,t)u + D(X,t)
$$

(4.34)

Where

$$D(X,t) = \Delta f(X,t) + \Delta J(X,t) + \Delta h(X,t)u + d(X,t) \tag{4.35}$$

The reference signal can be written as:

$$X_d = [x_d \ \dot{x}_d]^T = [V_{pv-ref} \ \dot{V}_{pv-ref}]^T \tag{4.36}$$

In the controller design, the tracking error are chosen by

$$\begin{cases} e_1 &= x_1 - x_d \\ e_2 &= \dot{e}_1 \\ e_2 &= x_2 - \dot{x}_d \\ \dot{e}_2 &= \dot{x}_2 - \ddot{x}_d \end{cases} \tag{4.37}$$

Sliding surface is defined as

$$s = k_1 e_1 + e_2 \tag{4.38}$$

$k_1 > 0$ is basically the design parameter. The derivation of Eq. 4.38 is given by

$$\dot{s} = k_1 e_2 + \dot{e}_2 \tag{4.39}$$

By combining Eq. 4.27 and Eq. 4.39 one can obtain

$$\dot{s} = k_1 e_2 + f(X,t) + J(X,t) + h(X,t) + D(X,t) - \ddot{x}_d \tag{4.40}$$

To calculate the control signal set $\dot{s} = 0$, the desired control law response is obtained as

$$\begin{aligned} u &= u_a + u_s \\ u_a &= h(X,t)^{-1}[\ddot{x}_d - f(X,t) - J(X,t) - c_1 e_2] - \hat{D}(X,t)] \\ u_s &= -h(X,t)^{-1} k_s sgn(s) \end{aligned} \tag{4.41}$$

Where $\hat{D}(X,t)$ is the estimation of $D(X,t)$, u_a is the adaptive compensation and u_s is the robust switching control item. k_s is the switching gain and $sgn(.)$ is the signum function defined as:

$$sgn(s) = \begin{cases} +1 & if s > 0 \\ 0 & if s = 0 \\ -1 & if s < 0 \end{cases} \tag{4.42}$$

4.3.2 Stability analysis

Lyapunov candidate function is used to prove the stability of the proposed control scheme []

$$V = \frac{1}{2}s^2 + \frac{1}{2\eta}\tilde{D}^2 \tag{4.43}$$

The sliding surface chosen in Eq.(4.38) is represented by s, $\tilde{D} = D - \hat{D}$ and $\eta > 0$ is adaptive law gain constant. We get the negative derivative of the Lyapunov candidate by taking the derivative of Eq.(4.43) which shows the control system is stable

$$\dot{V} = s\dot{s} + \frac{1}{\eta}\tilde{D}\dot{\hat{D}} \tag{4.44}$$

Putting $\dot{s}$ from Eq.(4.40) in Eq.(4.44) we get

$$\dot{V} = s(c_1 e_2 + f(X,t) + J(X,t) + h(X,t)u + D(X,t) - \ddot{x}) + \frac{1}{\eta}\tilde{D}\dot{\hat{D}} \tag{4.45}$$

Substituting the value of u from Eq.(4.41) in Eq.(4.45) and we obtain after simplification

$$\dot{V} = s(-k_s sgn(s) + (D(X,t) - \hat{D}(X,t)) + \frac{1}{\eta}\tilde{D}\dot{\hat{D}} \tag{4.46}$$

as $\tilde{D} = D - \hat{D}$ thus we have

$$\dot{V} = -k_s|s| + \tilde{D}S + \frac{1}{\eta}\tilde{D}\dot{\hat{D}} \tag{4.47}$$

Selecting the adaptive law as

$$\dot{\hat{D}} = -\eta s \tag{4.48}$$

It can be proved that $\dot{V} \leq 0$ when the switching gain $k_s > 0$ and closed loop system is stable.

Part III

SMC and Adaptive SMC application with different MPPT schemes

Chapter 5

Results and Discussions using SMC controller

In this chapter we discuss the simulation results obtained by implementing SMC controller employing P&O MPPT scheme for the proposed stand-alone PV system. Simulation results are first shown with classical proportional integral derivative (PID) controller for comparative study to validate the proposed controller performance. In the next section, results obtained using SMC control scheme are shown.

5.1   Simulation Results

Matlab/Simulink is used to model and simulate the proposed controller's technique. While the PV panel along with the boost converter and MPPT algorithm simulations are performed in PSIM (PowerSim), Simcoupler is used as an interface to couple Simulink and PSIM co-simulation. The parameters of the PV array that are used in this work are mentioned in Table. 5.1. From Table. 5.1, the short circuit current, open circuit voltage, and maximum power point tracking voltage of a single PV panel is given, for which a single DC-DC boost converter is selected. The parameters of the input capacitor and the inductor are selected such that the inductor current ripple equals to 1. A physical model of a PV panel is used according to the renewable energy module of PSIM [87], with parameters corresponding to the PV module of type MSX-60 [87]. Similarly, the parameters of the controller and converter are arranged in Table. 5.2. The design parameters of controllers are selected using Matlab optimization tools which are given in this Table. Simulations of the proposed controller are performed in PSIM and MATLAB/Simulink to verify its performance. The system is perturbed with an irradiance step of 1000W/m^2 in the instant 0 and after 50 ms,

Table 5.1 Parameters of the PV array.

Symbol	Parameter	Value
I_{sc}	Open circuit current	3.8 A
V_{oc}	Open circuit voltage	24V
I_{mp}	Maximum panel current	3.5 A
V_{mp}	Maximum panel voltage	17.1 V
$I_{s1} = I_{s2}$	Saturation currents	4.704×10^{-10}
I_{pv}	Panel current	3.8 A
R_{sh}	Shunt resistance	176.4 Ω
R_s	Series resistance	0.35 Ω

Table 5.2 Parameters of controller, converter, and maximum power point tracking (MPPT).

| Parameter	Value
L	22 μF
C	100 μF
V_o	24V
f_{sho}	49.9kHz
K_p	0.1
K_d	0.1
K_i	50
K_s(MPPT)	14.53
T_a	400 μF
ΔV_o	1 V
LPF	20kHz

LPF(low pass filter).

the irradiance is decreased by 50%. The irradiance is varied to validate the robustness of the proposed MPPT technique and temperature is kept constant at $25C^o$. The relationship coefficient of the Solar Panel MSX-60 used in the paper is $\pm0.05C^o$ m^2/W. This means that for an environment temperature of $25C^o$, the PV panel will operate up to $40C^o$ if irradiance is 1000 W/m^2, and $32.5C^o$ if irradiance is 500 W/m^2. Similarly, the temperature coefficient of power is $(0.5 \pm 0.15)\%/C^o$, which implies that maximum output power will be reduced to half if the irradiance level varies from maximum to half. The same effect is simulated in the study, and the irradiance level has been instantly reduced to 50% after 50 ms.

5.1.1   Response using the Proportional Integral Derivative (PID) Controller

To show the performance of the proposed SMC controller, it is compared with a conventional PID controller. The conventional controller response based on the P&O MPPT algorithm can be seen in Fig. 5.1, with a P&O perturbation amplitude of 1 V. The voltage tracking of the conventional controller is shown in Fig. 5.1a. Reference V_{ref} of the peak power voltage generated by P&O MPPT is successfully tracked by the PID controller. V_{ref} reaches the desired set point V_{ref} in a settling time of 5 ms. Fig. 5.1b shows the tracking error of the conventional controller with high ripples and oscillation. PV array output power along with the reference power curve is shown in Fig.5.1c. It can be observed that MPP is achieved by the conventional PID controller within 5 ms; however, it can be observed that the controller successfully tracks the reference but displays large ripples in the voltage waveform along with an overshoot. The zoomed views are provided in voltage and power curves to see the comparative behavior with reference voltage and power.
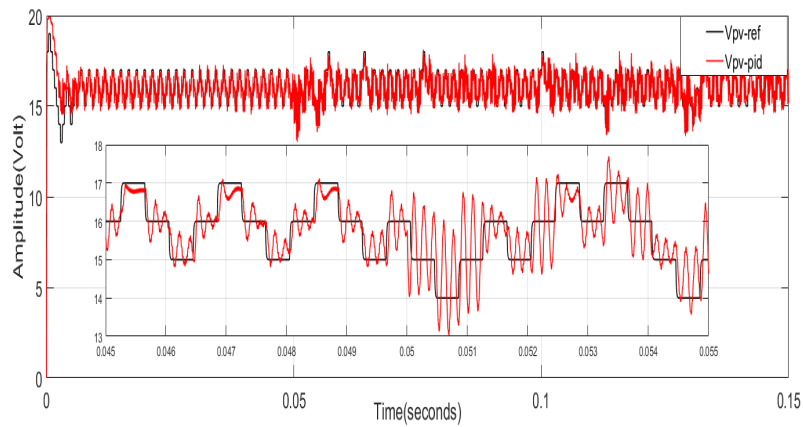
(a) Vpv-pid
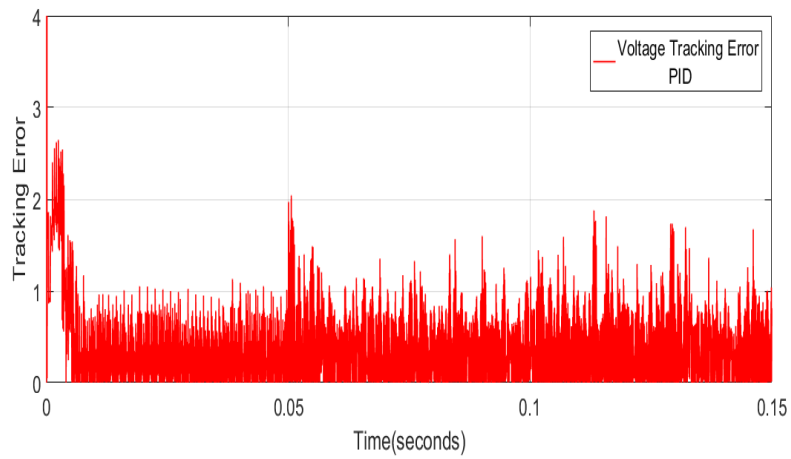
(b) Tracking-error-pid
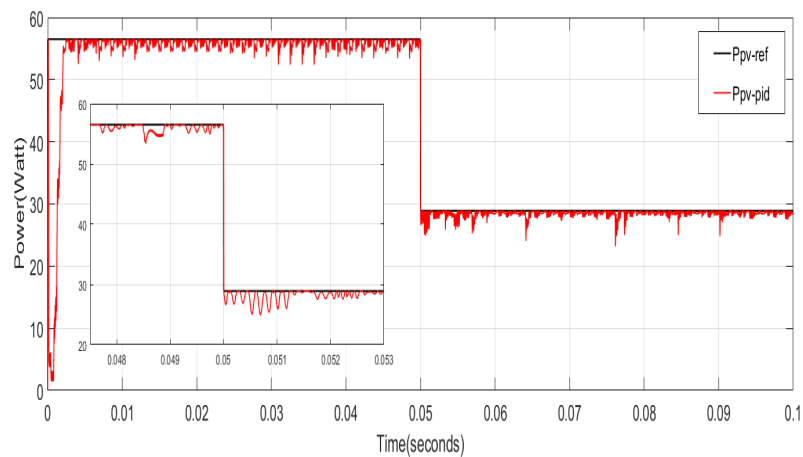
(c) Ppv-pid

Fig. 5.1 (a) Profile of the PV panel voltage, (b) tracking response of the proposed PID controller, and (c) profile of the PV power extraction.

5.1.2   Response using the Sliding Mode Controller (SMC) Controller

The output of the P&O-based MPPT is a voltage reference which needs to be tracked by the controller. The controller is used to keep track of the panel voltage with the reference voltage generated by P&O and ensuring a tracking error around 'zero' for the desired performance of the proposed controller. Fig. 5.2 shows the performance of the SMC controller based on the P&O algorithm with a perturbation amplitude of 1 V under variable irradiance. It can be seen in Fig. 5.2a that the panel voltage V_{pv} starts following the reference generated voltage V_{pv-ref} once it has reached the steady-state after transient behavior and successfully tracked the reference voltage. It is highlighted from the tracking response curve in Fig. 5.2b that the proposed controller clearly outperforms the conventional controller with little oscillation. During the abrupt variation of irradiance at 0.05 s, the controller performed well, showing the robustness of the controller. The proposed controller is not only robust, but the ripples are also negligible. Similarly, the PV panel output power along with the reference power curve is shown in Fig. 5.2c. It is observed that panel power P_{pv} and reference power V_{pv-ref} are following each other faster once they have reached the MPP. The efficiency of the system is greatly enhanced when the proposed controller is used. The results that are obtained by using an improved SMC controller are free of ripples and overshoot, but with PID, both of them are high and visible.

(a) Vpv-smc
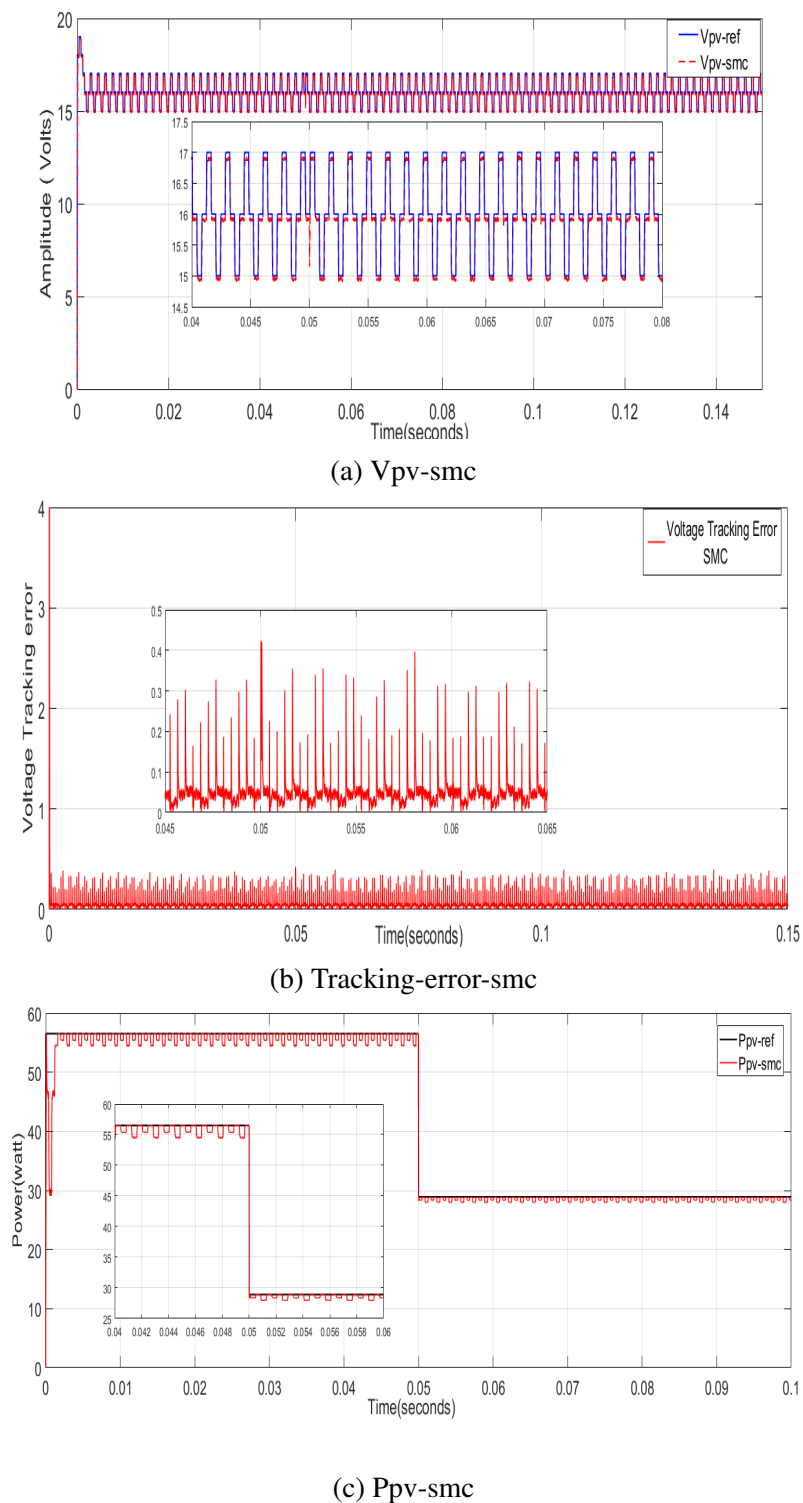

(b) Tracking-error-smc

(c) Ppv-smc

Fig. 5.2 (a) Profile of the PV panel voltage, (b) tracking response of the proposed SMC controller, and (c) profile of power extraction.

Table 5.3 Performance characteristics of the conventional PID and the proposed SMC controller.

Controller	Over/Undershoot(%)	Settling Time(s)	Power Losses (Watt)
PID	2.61	5 ms	3
SMC	0.6	0.3 ms	0.68

5.1.3   Comparative Analysis

Table. 6.1 shows that the overshoot characteristics, response time, and power losses have been explained. It is possible to deduct from Table. 6.1 that the performance characteristic parameters of the SMC controller in comparison with the PID controller for the proposed PV system have successfully improved. The comparison of the proposed SMC controller is done in below figures. In Fig. 5.3, the comparison of the proposed controller voltage curve is done with the reference signal and conventional controller voltage signal. Both controllers track the reference successfully, and there is high oscillation in the PID controller behavior. Similarly, Fig. 5.4 highlights the comparative behavior of the proposed controller panel power with reference signal power and conventional controller power. It can be observed that MPP is successfully achieved by the proposed SMC controller with almost negligible ripples compared to the PID controller, which has large ripples in correspondence to the reference signal. The zoomed views are also shown to clearly observe the comparison. The tracking error comparative plot is shown in Fig. 5.5, which shows high oscillations in the conventional controller response as compared to the proposed SMC controller which has little oscillations.
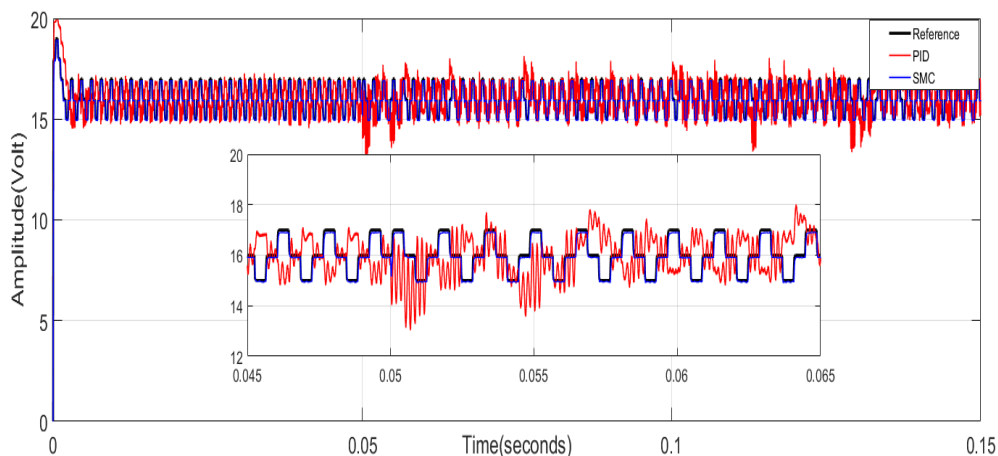

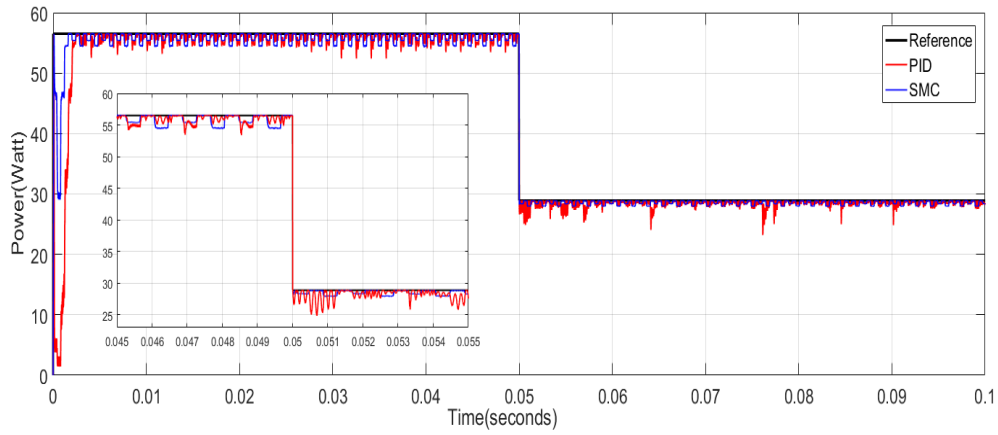Fig. 5.3 Reference, PID, and SMC PV voltage curve.
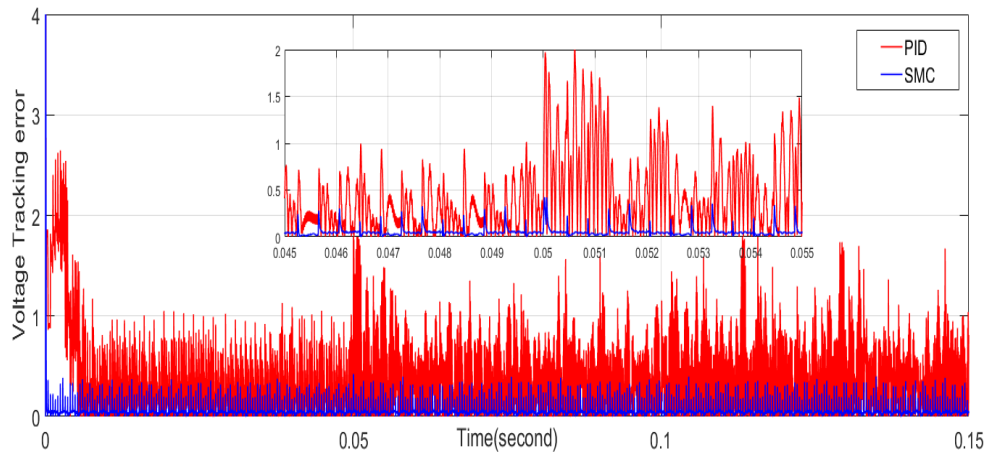
Fig. 5.4 Reference, PID, and SMC PV power curve.

Fig. 5.5 PID and SMC PV tracking error curve.

Chapter 6

Results and Discussions using Adaptive SMC controller

In this chapter, results obtained using adaptive SMC controller are discussed. Classical SMC generally suffers from the problem of 'Chattering', which is a very high frequency oscillation of the sliding variable around the sliding manifold. Adaptive SMC is introduced in this chapter which reduce chattering phenomenon and limit high frequency oscillations which was present in the results obtained using SMC shown in chapt.5. The previous study is conducted with only conventional P&O MPPT for reference sginal generation. In this chapter, we use two more MPPT algorithms (PSO,IPSM) along with P&O MPPT to provide reference signal to the controller. In general, IPSM optimization method is computationally efficient and offers the best solution than the other optimization algorithms PSO and P&O. To test the performance of the proposed adaptive SMC controller, the results are compared with the classical PID controller to show the significance of the adopted control scheme.

6.1   Simulation Results and Discussion

In this section, the results for each one of the three MPPT implemented algorithms are shown. The description of the irradiance experiment as well as parameters for the PV system are described in details in Section 5.1. The same parameters of the PV array are used in this study. The parameters of the controller and converter are arranged in Table 6.1. MATLAB optimization tools are used to obtain the design parameters of controllers which are displayed additionally in this table. The system is perturbed with an irradiance step of 1000W/m^2 at the instant 0 and after 50 ms the irradiance is decreased by 50% for an environment temperature of 25C^o.

Table 6.1 Parameters of controller, converter, and MPPT.

| Parameter	Value
L	22 μF
C	100 μF
V_o	24V
f_{sho}	49.9kHz
K_p	0.1
K_I	50
K_d	0.1
K_1	4.3
K_A	55.5
T_a	400 μF
ΔV_o	1 V(P&O)
ΔV_o	0.2 V(40 p.)
ΔV_o	0.8 V(10 p.)
LPF	20kHz

LPF(low pass filter).

6.1.1 Response using PID
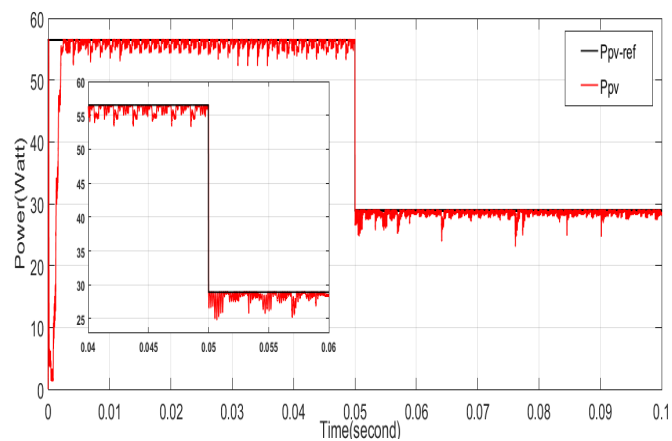
a) with P&O MPPT scheme

To show the performance of the proposed chattering-free adaptive SMC controller, it is compared with a conventional PID controller. PID controller tuning parameters have been obtained by using MATLAB/Simulink optimization tools. The conventional controller response based on the P&O MPPT can be seen in Fig. 6.1, with a P&O perturbation amplitude of 1 V. The output of P&O MPPT is a voltage reference signal which is supposed to be tracked by controller to ensure tracking error around zero. Fig. 6.1a is the PV panel voltage which is tracked by controller with reference voltage. V_{pv} successfully tracks V_{ref} once reached steady state after transient behaviour. But the V_{pv} deviates from V_{ref} in PID controller. Fig. 6.1b shows the tracking error of the conventional controller. There is high ripples and oscillations in PID tracking error behavior. PV panel output power along with reference power curve is shown in Fig. 6.1c. From power curve it can be seen that MPP is achieved successfully and the controller tracks the reference voltage in the voltage curve but displays large ripples in the voltage waveform along with an overshoot.
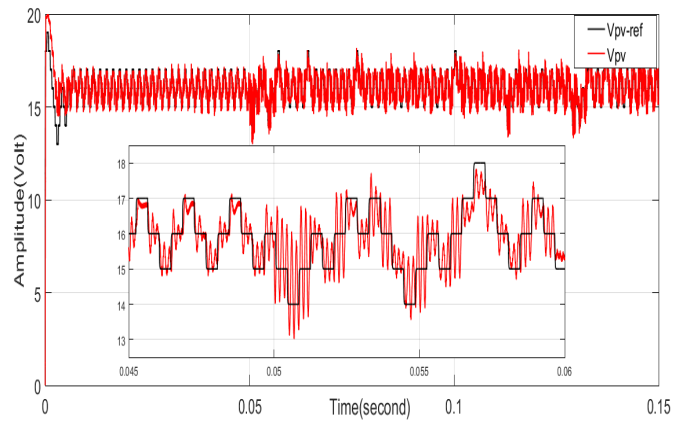
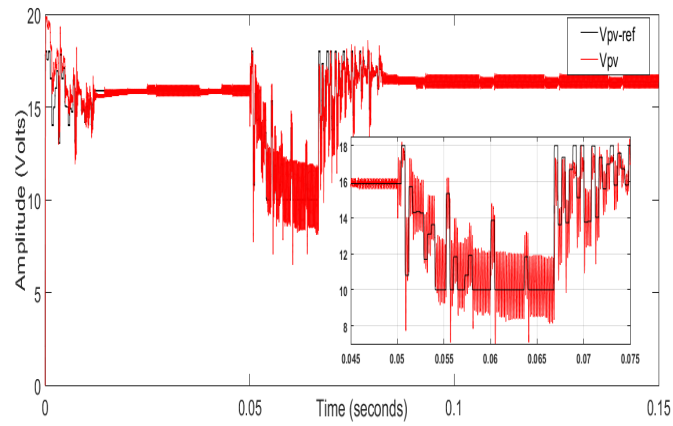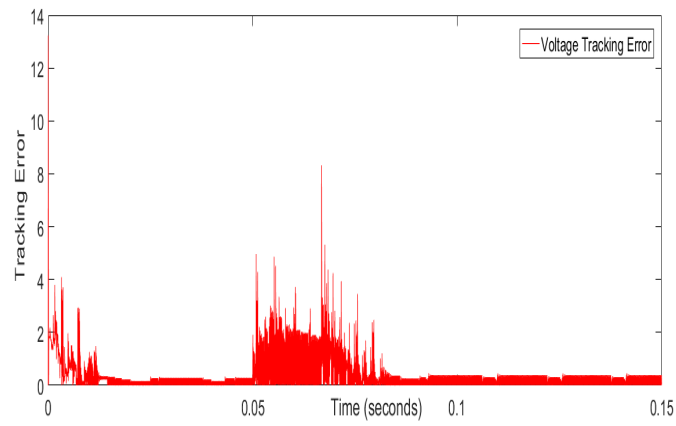(a) Vpv-pid-p&o
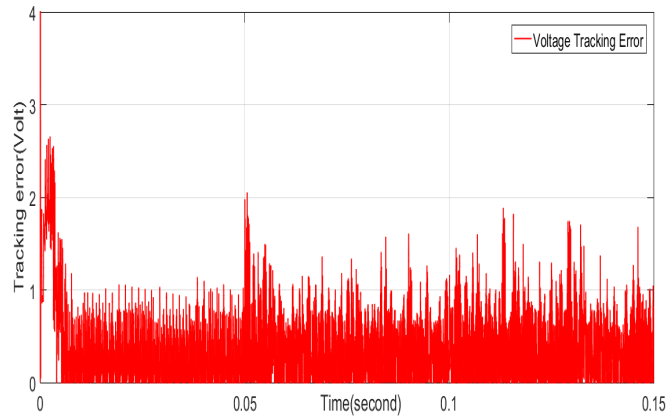
(b) Tracking-error

(c) Ppv-pid-p&o

Fig. 6.1 PID based on P&O MPPT (a) Profile of the PV panel voltage (b) Tracking response (c)Profile of the PV power extraction

b) with PSO MPPT scheme

The conventional controller response based on PSO MPPT can be seen in Fig. 6.2 and Fig. 6.3. As a stochastic algorithm, PSO does not always guarantee the same exact location for the best positioned particle (optimal solution). Therefore, a set of 10 simulations have been conducted. Each simulation set has been repeated by suing 10 and 40 particles. From the PSO with 10 particles plots it can be observed that the panel voltage is tracked by the controller with the reference voltage in Fig. 6.2a and the panel power reached the MPP in the power curve Fig. 6.2c. The tracking error response is shown in Fig. 6.2b with less oscillations and ripples as compared to P&O MPPT based results. However, the response of PSO algorithm with 40 particles in Fig. 6.3 never reached the steady-state MPP unlike the response based on PSO with 10 particles and particles always moving around the search-space. The oscillations are significant in PID responses. As a result, it can be seen that PSO generated reference voltages, incurred in large oscillations, therefore energy loses. Also, in some situations, difficulties to appropriately reach the steady state.
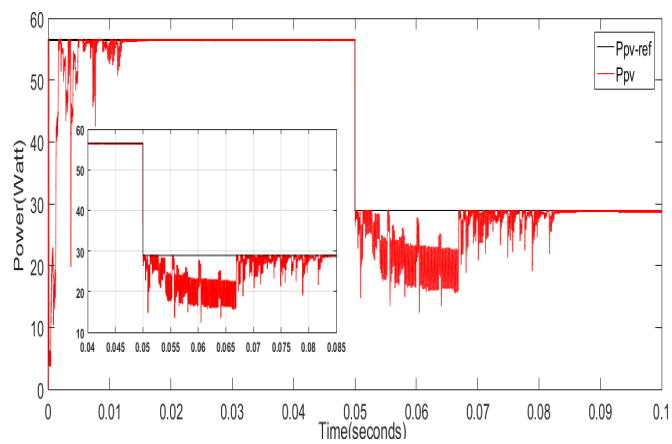
(a) Vpv-pid-pso10

(b) Tracking-error-pidpso10

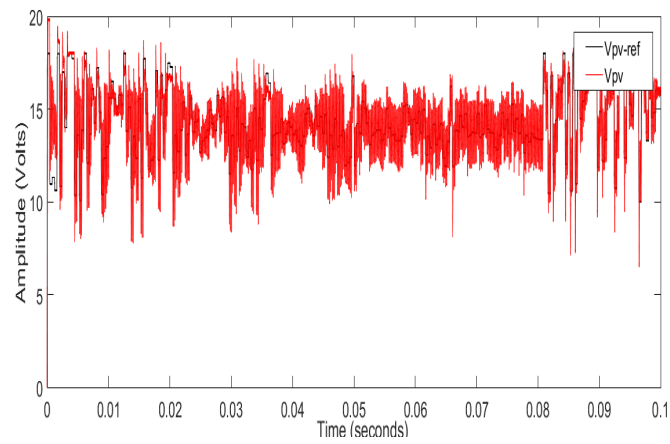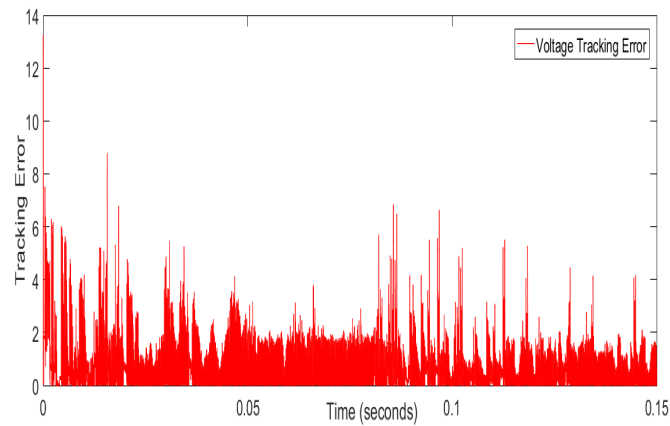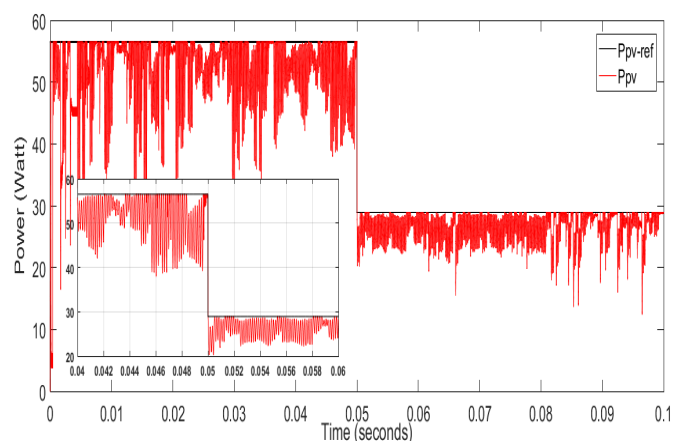
(c) Ppv-pid-pso10

Fig. 6.2 PID based in PSO MPPT with 10 particles (a) Profile of the PV panel voltage (b) Tracking response (c)Profile of the PV power extraction
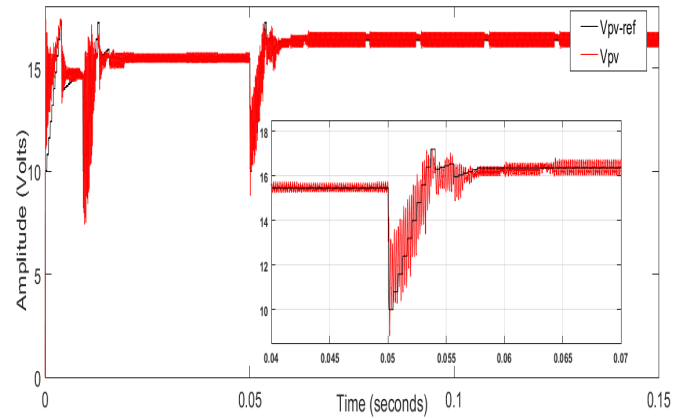
(a) Vpv-pid-pso40

(b) Tracking-error-pidpso40

(c) Ppv-pid-pso40

Fig. 6.3 PID based in PSO MPPT with 40 particles (a)Profile of the PV panel voltage
(b)Tracking response (c)Profile of the PV power extraction

c) with IPSM MPPT scheme

In this section, the MPPT algorithm based on Improved PSM will be tested. As in the preceding section, because the algorithm is of stochastic nature, two sets of 10 simulations each will be pursued. One with 10 models and a second one with 40 models. Results are shown in Figs. 6.4 & Fig. 6.5, respectively. This optimization method is computationally efficient to observe the best solution than the PSO optimization method. IPSM with 10 and 40 models converge faster than the PSO with 10 and 40 particles. The perturbation amplitude is greater when the number of models will be low or vice versa to reach to the optimal solution. From the voltage curves (Fig.6.4a, Fig. 6.5a) the conventional controller tracks the panel voltage successfully with reference voltage; PID voltage curve deviates from reference voltage and has great oscillations. The power curves reach the MPP shown in Fig. 6.4c & Fig. 6.5c. The tracking error curves (Fig. 6.4b & Fig. 6.5b) show minimized tracking error behaviour as compared to PSO based MPPT tracking response.

(a) Vpv-pid-ipsm10

(b) Tracking-error-ipsm10

(c) Ppv-pid-ipsm10

Fig. 6.4 PID based in IPSM MPPT with 10 particles (a) Profile of the PV panel voltage (b) Tracking response (c)Profile of the PV power extraction

(a) Vpv-pid-ipsm40

(b) Tracking-error-ipsm40
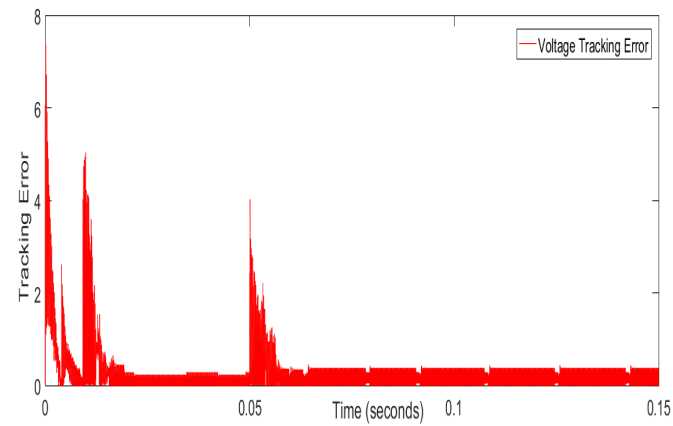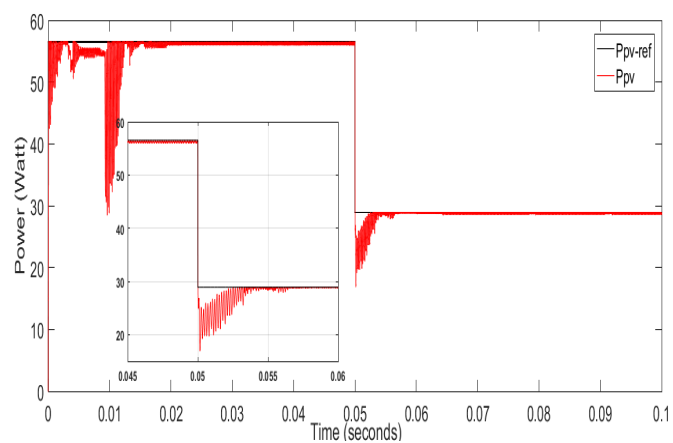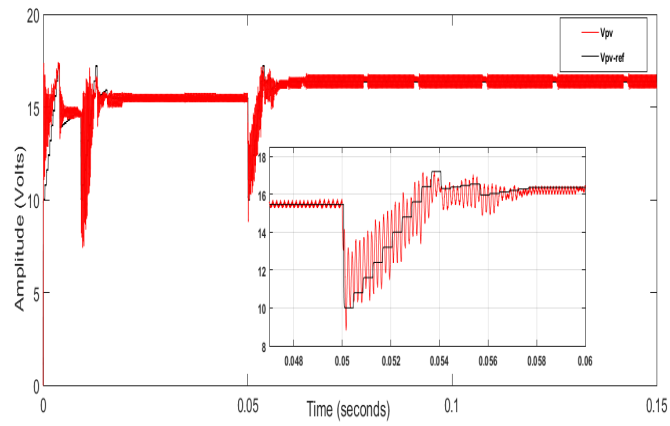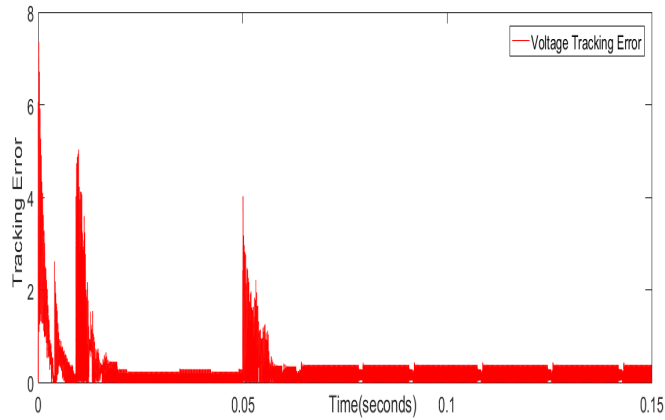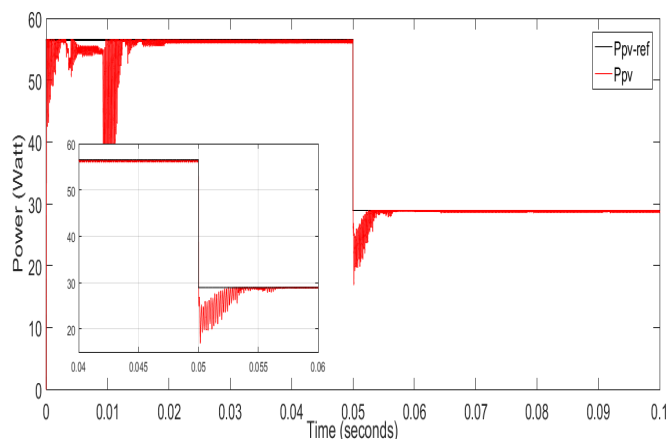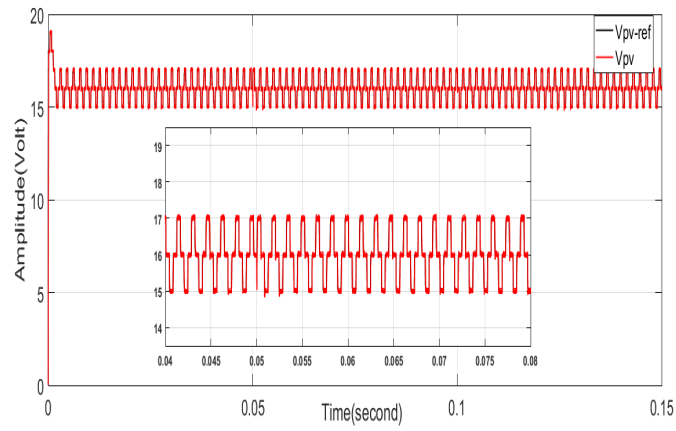

(c) Ppv-pid-ipsm40

Fig. 6.5 PID based in IPSM MPPT with 40 particles (a)Profile of the PV panel voltage (b)Tracking response (c)Profile of the PV power extraction

6.1.2   Response using Adaptive SMC

a) with P&O MPPT scheme

In this section the performance of the ASMC controller is discussed which is introduced to limit the chattering effect,to keep tracking of the panel voltage with the reference voltage generated by MPPT algorithms and ensuring a tracking error around 'zero' for the desired response. Fig. 6.6 shows the performance of the ASMC controller based on the P&O algorithm with a perturbation amplitude of 1 V under varaible irradiance. It can be seen in Fig. 6.6a that the panel voltage V_{pv} starts following the reference-generated voltage V_{ref} once it has reached the steady-state after transient behavior and successfully tracked the reference voltage. Also there is no deviation in the proposed controller PV voltage. It is highlighted from the tracking response curve in Fig. 6.6b that the proposed controller clearly outperforms the conventional controller with little oscillation. During the abrupt variation of irradiance at 0.05 s, the controller performed well, showing the robustness of the controller. The proposed controller is not only robust, but the ripples are also negligible. Similarly, the PV panel output power along with the reference power curve is shown in Fig. 6.6c. It is observed that panel power P_{pv} and reference power P_{pv-ref} are following each other faster once they have reached the MPP. The results that are obtained by using adaptive SMC are free of high frequency oscillations.

(a) Vpv-asmc-pndo
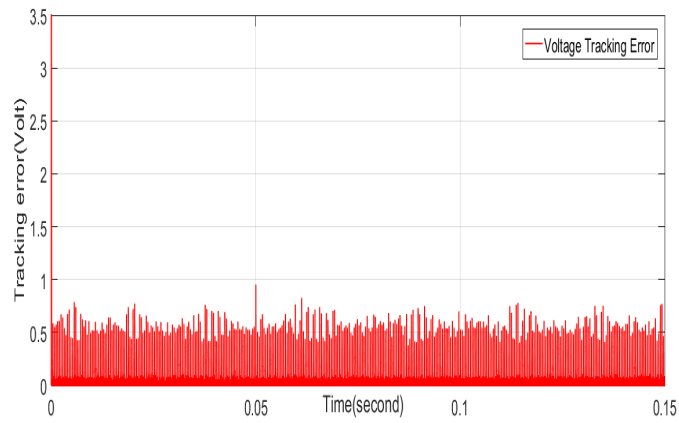
(b) Tracking-error-p&o
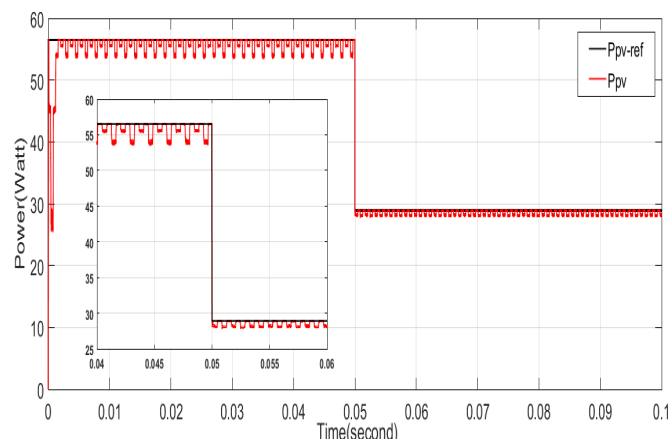
(c) Ppv-asmc-pndo

Fig. 6.6 ASMC based on P&O MPPT (a) Profile of the PV panel voltage (b) Tracking response (c)Profile of the PV power extraction

b) with PSO MPPT scheme

The adaptive SMC response based on PSO MPPT can be seen in Fig. 6.7 and Fig. 6.8. A set of 10 simulations have been conducted. Each simulation set has been repeated by using 10 and 40 particles. The controller tracks the reference V_{ref} successfully of the panel voltage in PSO with 10 particles in Fig. 6.7a. Fig. 6.7b shows the tracking error response with limited oscillations as compared to P&O MPPT based results. In the power curve Fig. 6.7c, the algorithm reached the MPP successfully. PSO with 10 particles shows average response and the algorithm reached the MPP before the simulation ended. However, the behavior using ASMC shows limited oscillations and less ripples in comparison of PID. On the other hand, the response of PSO algorithm with 40 particles in Fig. 6.8 never reached the steady state and always keeps moving around the search-space. However, with adaptive SMC the oscillations reduced in the performance of PSO with 40 particles, which are significant in PID.
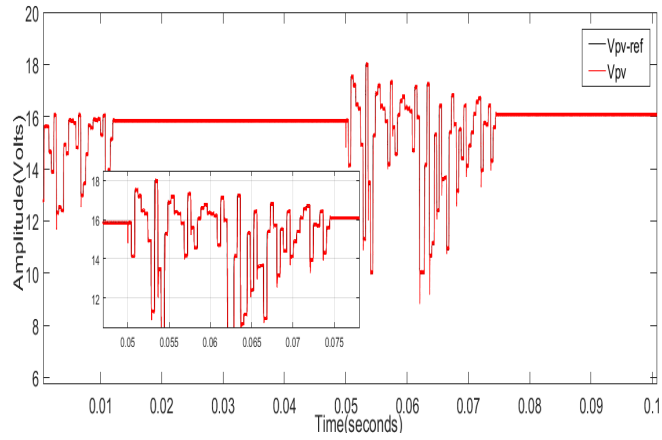
(a) Vpv-asmc-pso10

(b) Tracking-error-pso10

(c) Ppv-asmc-pso10

Fig. 6.7 ASMC based in PSO MPPT with 10 particles (a) Profile of the PV panel voltage (b) Tracking response (c)Profile of the PV power extraction

(a) Vpv-asmc-pso40

(b) Tracking-error-pso40

(c) Ppv-asmc-pso40

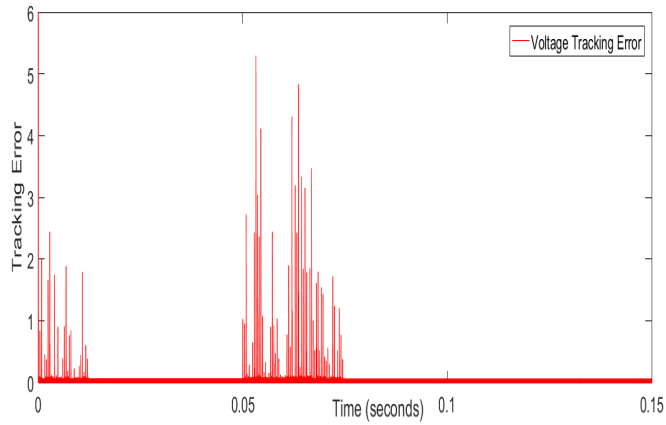Fig. 6.8 ASMC based in PSO MPPT with 40 particles (a)Profile of the PV panel voltage (b)Tracking response (c)Profile of the PV power extraction

c) with IPSM MPPT scheme

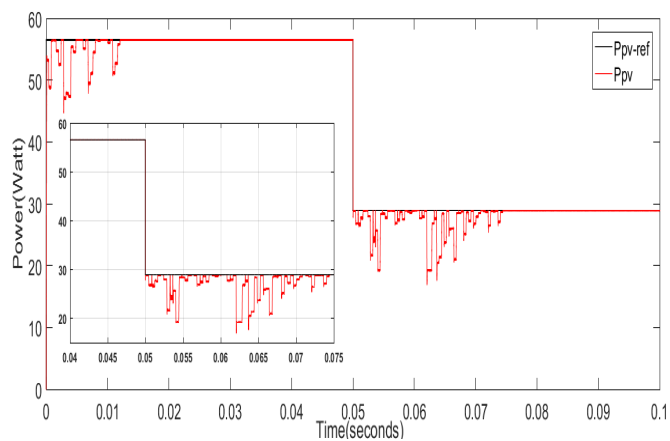In this section, the MPPT algorithm based on Improved PSM will be tested. The algorithm is of stochastic nature, two sets of 10 simulations each will be pursued with ASMC also. One with 10 models and a second one with 40 models. This optimization method is computationally efficient to observe the best solution than the PSO optimization method. This optimization method converge faster than the previous one with 10 and 40 models. The perturbation amplitude is greater when the number of models will be low or vice versa to reach to the optimal solution. It is cleared from the plots given below that the proposed ASMC controller based on IPSM MPPT has negligible ripples and no deviation from MPP in obtained voltage and power curves. The panel voltage tracks the reference voltage in Fig. 6.9a & 6.10a successfully once reached the steady state. The tracking response curves in Fig. 6.9b & 6.10b highlight that the adaptive controller clearly outperforms the conventional PID controller and the curves show minimized tracking error behavior as compared to PSO MPPT tracking response oscillations. It can be observed that MPP is successfully achieved in PV array output power curves which are shown in Fig. 6.9c & 6.10c, with negligible ripples compared to other MPPT techniques with ASMC controller. As main feature to highlight from the IPSM based MPPT algorithm in comparison with the previously presented ones, is that it takes some more time to get the MPP but it guarantees to reach it. Also, it exhibits less power energy loses rather than the PSO. In this manner, the validation of the chattering free and robustness of the proposed adaptive sliding mode controller based on IPSM MPPT under variable environmental conditions and uncertainities is validated by comparing its performance with conventional controller based on P&O and PSO MPPT algorithms.

(a) Vpv-asmc-ipsm10
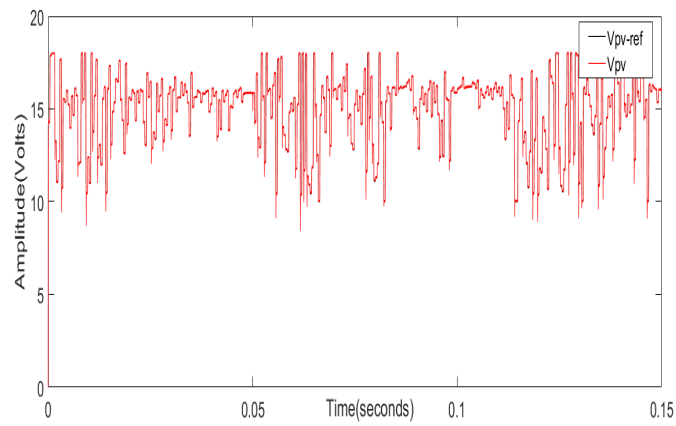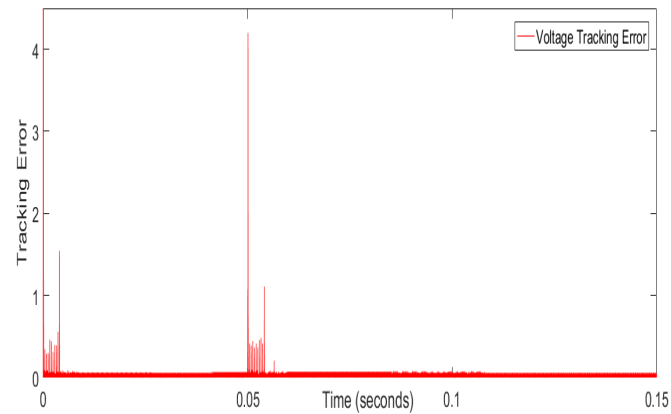

(b) Tracking-err-ipsm10

(c) Ppv-asmc-ipsm10

Fig. 6.9 ASMC based in IPSM MPPT with 10 particles (a) Profile of the PV panel voltage (b) Tracking response (c)Profile of the PV power extraction
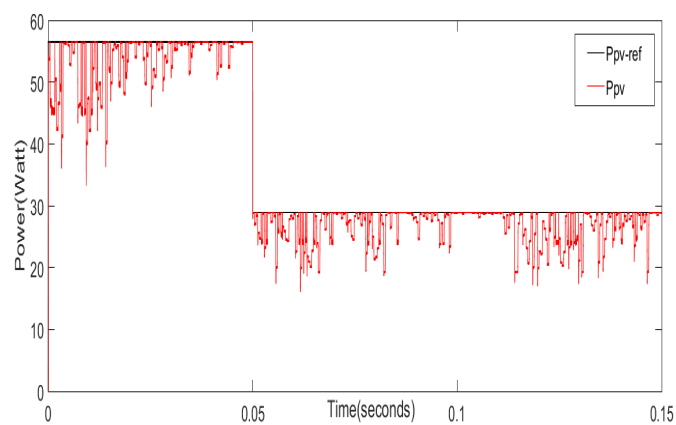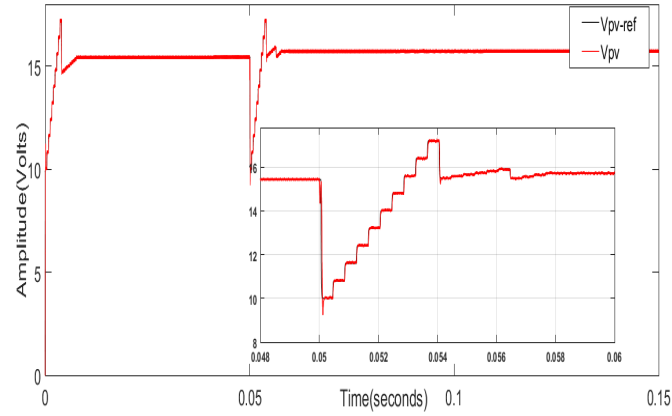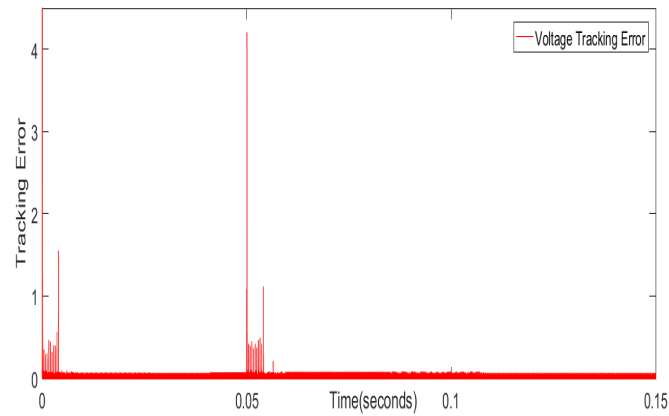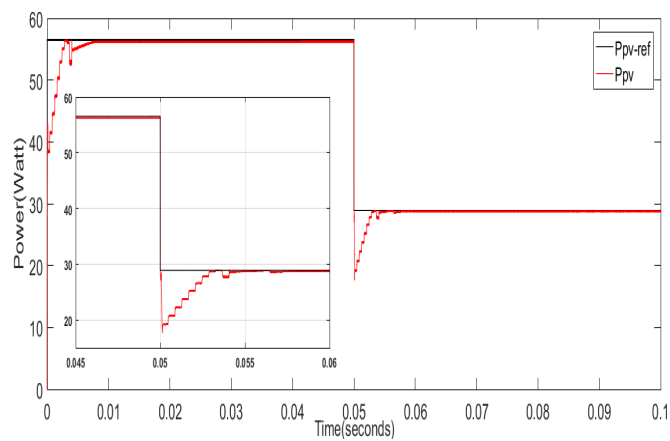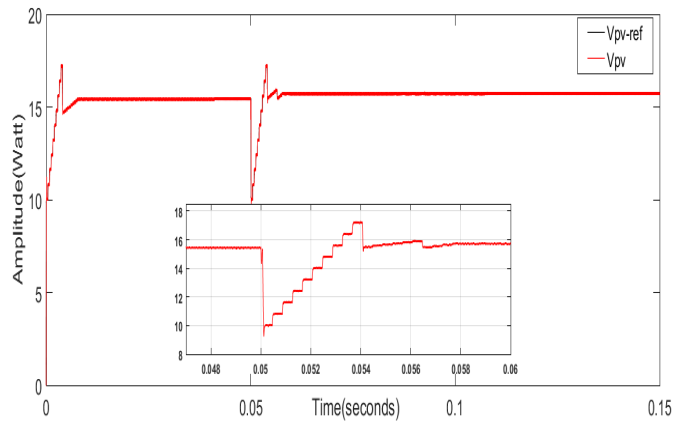
(a) Vpv-asmc-ipsm40
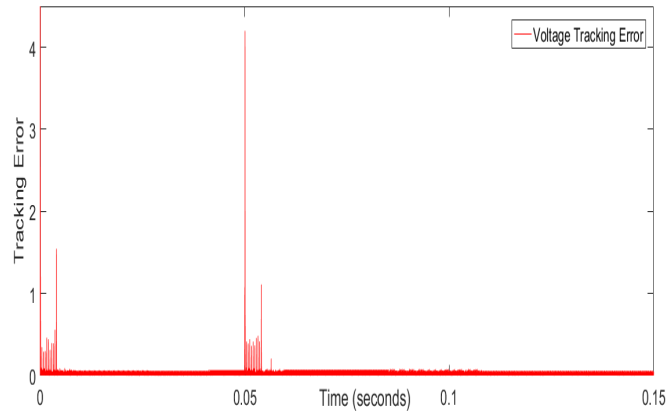
(b) Tracking-err-ipsm40
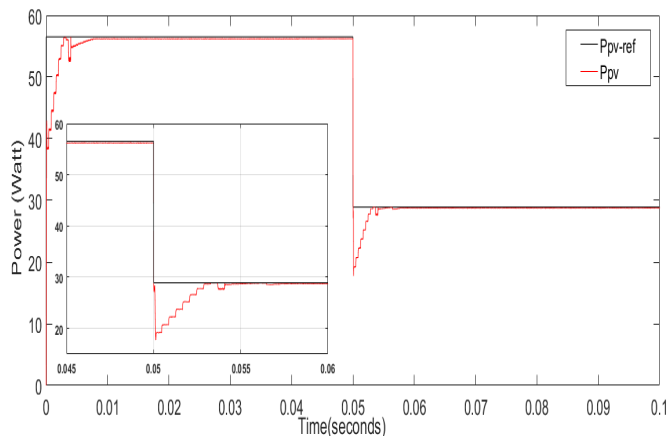
(c) Ppv-asmc-ipsm40

Fig. 6.10 ASMC based in IPSM MPPT with 40 particles (a)Profile of the PV panel voltage (b)Tracking response (c)Profile of the PV power extraction

6.1.3   Discussion

From the previous three MPPT scenarios with PID and ASMC controllers, IPSM MPPT algorithm provides an overall satisfactory response. As a resume quantitative comparison, the performance characteristics parameters of the proposed ASMC controller in comparison with the conventional PID controller are discussed in this section with employed MPPT schemes. The performance characteristics are shown in provided tables which describe the overshoot characteristic, response time, and power losses. These tables show the different considered figures of merit. Clear advantages of the tested optimization based MPPT algorithms over traditional P&O have been shown in these tables. In both cases PSO and IPSM, 10 and 40 particle optimizations have been conducted. Regarding IPSM, as shown in Tables. 6.5 and 6.6, ASMC results are similar in both cases (10 and 40 particles) and superior in speed of response and power loses to the PSO ones (IPSM shows to be 2 times faster and exhibits half power loses). It is worth to mention that for the ASMC based P&O MPPT algorithm, it provides reasonable performance indicators, even aligned with the PSO based MPPT but even faster from the settling time point of view (see Tables 6.2–6.4). In the case of the IPSM, the settling time is greatly improved with respect to PSO and made overall better results with respect to the original P&O. IPSM therefore, is providing a good alternative as MPPT algorithm. Next the performance of the proposed ASMC controller is depicted by determining the aggregated error index, IAE. This aggregated index, confirms this approach ASMC controller with IPSM provides better performance than the other implemented MPPT techniques.Fig. 6.11 show the comparative plots of the performance index IAE (Integral Absolute Error) of the PV system. The performance index, IAE, shows that the IPSM technique is performing better than the ones based on P&O and PSO MPPT algorithms.

Table 6.2 Performance characteristics of the conventional controller and the proposed ASMC controller based on P&O MPPT.

Controller	Over/Undershoot(%)	Settling Time(s)	Power Losses (Watt)
PID	2.8	5.3 ms	3.2
ASMC	0.6	0.15 ms	0.68

Table 6.3 Performance characteristics of the conventional controller and the proposed ASMC controller based on PSO 10 particles.

Controller	Over/Undershoot(%)	Settling Time(s)	Power Losses (Watt)
PID	8	80 ms	6
ASMC	0.85	2.8 ms	0.95

Table 6.4 Performance characteristics of the conventional controller and the proposed ASMC controller based on PSO 40 particles.

Controller	Over/Undershoot(%)	Settling Time(s)	Power Losses (Watt)
PID	10	120 ms	7.8
ASMC	1	3 ms	1.2

Table 6.5 Performance characteristics of the conventional controller and the proposed ASMC controller based on IPSM 10 particles.

Controller	Over/Undershoot(%)	Settling Time(s)	Power Losses (Watt)
PID	5	50 ms	4.8
ASMC	0.40	0.10 ms	0.54

Table 6.6 Performance characteristics of the conventional controller and the proposed ASMC controller based on IPSM 40 particles.

Controller	Over/Undershoot(%)	Settling Time(s)	Power Losses (Watt)
PID	5.8	53 ms	5.2
ASMC	0.41	0.11 ms	0.59
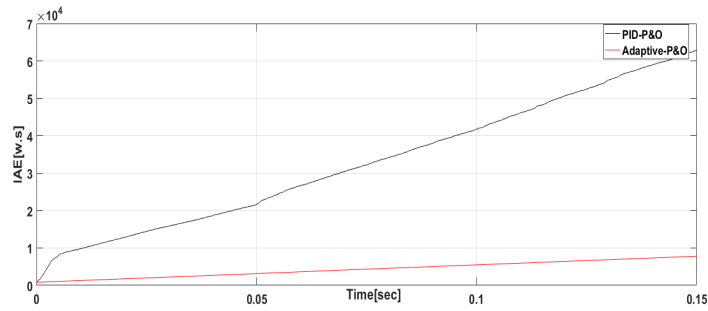
(a) IAE-p&o
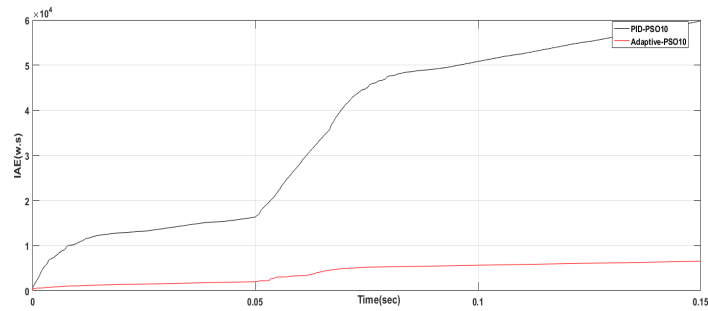
(b) IAE-pso10
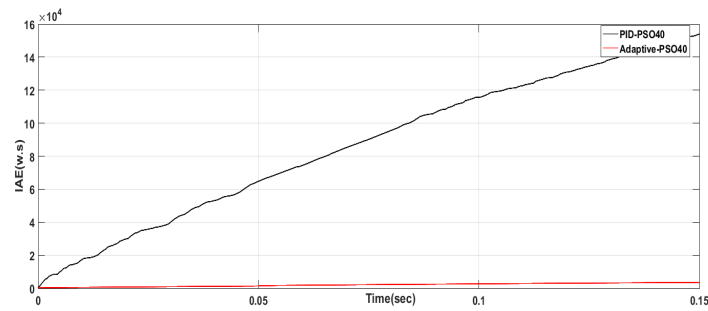
(c) IAE-pso40
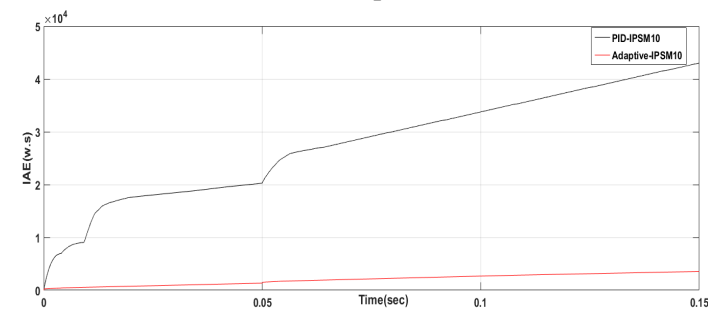
(d) IAE-ipsm10
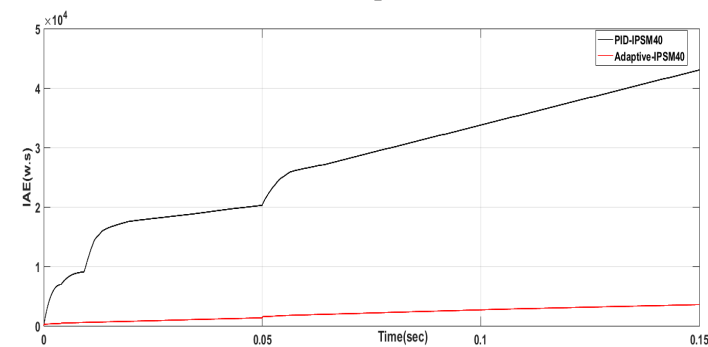
(e) IAE-ipsm40

Fig. 6.11 Integral Absolute Erros, IAE performance index

Part IV

Conclusions and perspectives

Chapter 7

Conclusions and Future Work

In this chapter, we conclude the thesis by summarizing our main contributions and presenting the future lines of research related to the contributions of this thesis.

7.1 Overall Conclusions

In this thesis, we studied the modeling of the sliding mode controller of photovoltaic system by employing MPPT schemes. SMC controllers are used for the extraction of maximum power from PV source. We developed two-loop control scheme for maximization of the power from PV source. Based on the work done to achieve the main objectives, the overall conclusions of this thesis are summarized as follows:

- First, we studied the fundamentals of the photovotlaic system and several components of stand-alone PV system. We studied further in details different components of PV system i.e. solar panel, single diode model and two diode model of solar cell, power electronic converter topologies. We presented techniques available in the literature for maximum power extraction of PV and studied numerous MPPT techniques which consist of Conventional Techniques, Soft Computing Technique, Linear & Non Linear control techniques for power extraction from PV.

- Second, we proposed sliding mode controller and adaptive sliding model controller in this thesis for power extraction from PV based on MPPT schemes. SMC controller background and theory has been discussed. Some non-linear system dynamic has been derived using SMC and stability has been checked. Further to show the behaviour of SMC; simulation results have been shown in MATLAB to show the robustness of the controller. Further adaptive SMC mathematical model is developed for the same non linear system and stability is checked. Simulation results were shown.

- Third, we presented and derived the mathematical model of the integer order classical SMC controller for our propsoed PV system. Derivation of SMC controller is developed for PV with MPPT scheme and stability is proved. P&O MPPT algorithm is used to generate the reference signal. The reference signal provided to the controller for tracking of the panel voltage. The controller is used to track the voltage signals for maximization of power and achieved MPP successfully. From the obtained results controller performance has been validated by comparing its performance with conventional PID controller in terms of voltage tracking, power curves and tracking error. Performance characteristics parameters have been estimated in tabular form for both controllers in terms of overshoot/undershoot, settling time and power losses.

- Lastly, we presented adaptive SMC controller for our system to deal with the chattering effect which was present in SMC. Controller mathematical model is developed based on boost converter dynamics. Stability is validated of the developed control scheme for the system. Along with P&O two other MPPT optimization algorithms PSO and IPSM were employed with ASMC for reference signal generation. IPSM MPPT scheme provided an overall satisfactory response from the other PSO optimization scheme and the traditional P&O. The obtained results compared with the classical PID controller to highlight the significance of the developed ASMC control scheme. The results verified the controller performance.

7.2   Future Work

We believe that the main contributions of our work can be extended to further work in relation to the contributions of this thesis. There are always improvements or extensions which can be addressed to continue working. The more advanced control schemes super twisting SMC, terminal SMC and fractional SMC can be implemented for the same system to represent our future work. Experimental validation of the simulation results can be performed leading to practical implementation of the proposed work.

References

[1] P. Ekins, M. J. Bradshaw, and J. Watson, *Global energy: Issues, potentials, and policy implications*. Oxford University Press, 2015.

[2] A. Poullikkas, *Renewable Energy: Economics, Emerging Technologies, and Global Practices*. Nova Science Publishers, 2013.

[3] R. Wengenmayr and T. Bührke, *Renewable energy: sustainable energy concepts for the future*. John Wiley & Sons, 2011.

[4] R. Sims, "Energy for tomorrow's world. a renewable energy perspective," *Renewable Energy World*, vol. 3, no. 4, pp. 24–30, 2000.

[5] R. A. Messenger and A. Abtahi, *Photovoltaic systems engineering*. CRC press, 2017.

[6] F. Mehmood, N. Ashraf, L. Alvarez, T. N. Malik, H. K. Qureshi, and T. Kamal, "Grid integrated photovoltaic system with fuzzy based maximum power point tracking control along with harmonic elimination," *Transactions on Emerging Telecommunications Technologies*, p. e3856, 2020.

[7] C. Mehdipour and F. Mohammadi, "Design and analysis of a stand-alone photovoltaic system for footbridge lighting," *Journal of Solar Energy Research*, vol. 4, no. 2, pp. 85–91, 2019.

[8] M. A. G. De Brito, L. Galotto, L. P. Sampaio, G. d. A. e Melo, and C. A. Canesin, "Evaluation of the main mppt techniques for photovoltaic applications," *IEEE transactions on industrial electronics*, vol. 60, no. 3, pp. 1156–1167, 2012.

[9] R. A. Cullen, "What is maximum power point tracking (mppt) and how does it work?" *Blue Sky Energy*, vol. 16, 2000.

[10] S. Balakrishna, N. A. Thansoe, G. Rajamohan, and C. Ling, "The study and evaluation of maximum power point tracking systems," in *International Conference on Energy and Environment*, pp. 17–22.

[11] J. P. Ram, T. S. Babu, and N. Rajasekar, "A comprehensive review on solar pv maximum power point tracking techniques," *Renewable and Sustainable Energy Reviews*, vol. 67, pp. 826–847, 2017.

[12] N. Karami, N. Moubayed, and R. Outbib, "General review and classification of different mppt techniques," *Renewable and Sustainable Energy Reviews*, vol. 68, pp. 1–18, 2017.

[13] M. Sivagamasundari, P. M. Mary, and V. Velvizhi, "Maximum power point tracking for photovoltaic system by perturb and observe method using buck boost converter," *International Journal of Advanced Research in Electrical, Electronics and Instrumentation Engineering*, vol. 2, no. 6, pp. 2433–2439, 2013.

[14] D. Sera, L. Mathe, T. Kerekes, S. V. Spataru, and R. Teodorescu, "On the perturb-and-observe and incremental conductance mppt methods for pv systems," *IEEE journal of photovoltaics*, vol. 3, no. 3, pp. 1070–1078, 2013.

[15] S. Titri, C. Larbes, K. Y. Toumi, and K. Benatchba, "A new mppt controller based on the ant colony optimization algorithm for photovoltaic systems under partial shading conditions," *Applied Soft Computing*, vol. 58, pp. 465–479, 2017.

[16] A. Ali, K. Almutairi, M. Z. Malik, K. Irshad, V. Tirth, S. Algarni, M. Zahir, S. Islam, M. Shafiullah, N. K. Shukla *et al.*, "Review of online and soft computing maximum power point tracking techniques under non-uniform solar irradiation conditions," *Energies*, vol. 13, no. 12, p. 3256, 2020.

[17] A. Bahgat, N. Helwa, G. Ahmad, and E. El Shenawy, "Maximum power point traking controller for pv systems using neural networks," *Renewable Energy*, vol. 30, no. 8, pp. 1257–1268, 2005.

[18] L. P. Sampaio, M. V. da Rocha, S. A. O. da Silva, and M. H. T. de Freitas, "Comparative analysis of mppt algorithms bio-inspired by grey wolves employing a feed-forward control loop in a three-phase grid-connected photovoltaic system," *IET Renewable Power Generation*, vol. 13, no. 8, pp. 1379–1390, 2019.

[19] I. Purnama, Y.-K. Lo, and H.-J. Chiu, "A fuzzy control maximum power point tracking photovoltaic system," in *2011 IEEE International Conference on Fuzzy Systems (FUZZ-IEEE 2011)*. IEEE, 2011, pp. 2432–2439.

[20] L. M. Elobaid, A. K. Abdelsalam, and E. E. Zakzouk, "Artificial neural network-based photovoltaic maximum power point tracking techniques: a survey," *IET Renewable Power Generation*, vol. 9, no. 8, pp. 1043–1063, 2015.

[21] A. A. Kulaksız and R. Akkaya, "A genetic algorithm optimized ann-based mppt algorithm for a stand-alone pv system with induction motor drive," *Solar Energy*, vol. 86, no. 9, pp. 2366–2375, 2012.

[22] I. Ferdiansyah, S. Sutedjo, O. A. Qudsi, and A. N. Ramadhan, "Implementation of maximum power point tracking on solar panels using cuckoo search algorithm method," in *2019 2nd International Conference on Applied Information Technology and Innovation (ICAITI)*. IEEE, 2019, pp. 88–92.

[23] A. Besheer and M. Adly, "Ant colony system based pi maximum power point tracking for stand alone photovoltaic system," in *2012 IEEE International Conference on Industrial Technology*. IEEE, 2012, pp. 693–698.

[24] H. Renaudineau, F. Donatantonio, J. Fontchastagner, G. Petrone, G. Spagnuolo, J.-P. Martin, and S. Pierfederici, "A pso-based global mppt technique for distributed pv power generation," *IEEE Transactions on Industrial Electronics*, vol. 62, no. 2, pp. 1047–1058, 2014.

[25] M. F. N. Tajuddin, S. M. Ayob, Z. Salam, and M. S. Saad, "Evolutionary based maximum power point tracking technique using differential evolution algorithm," *Energy and Buildings*, vol. 67, pp. 245–252, 2013.

[26] M. Y. Javed, A. F. Murtaza, Q. Ling, S. Qamar, and M. M. Gulzar, "A novel mppt design using generalized pattern search for partial shading," *Energy and Buildings*, vol. 133, pp. 59–69, 2016.

[27] C. Audet, "Convergence results for generalized pattern search algorithms are tight," *Optimization and Engineering*, vol. 5, no. 2, pp. 101–122, 2004.

[28] S. Veerapen, H. Wen, and Y. Du, "Design of a novel mppt algorithm based on the two stage searching method for pv systems under partial shading," in *2017 IEEE 3rd International Future Energy Electronics Conference and ECCE Asia (IFEEC 2017-ECCE Asia)*. IEEE, 2017, pp. 1494–1498.

[29] F. F. Ahmad, C. Ghenai, A. K. Hamid, and M. Bettayeb, "Application of sliding mode control for maximum power point tracking of solar photovoltaic systems: A comprehensive review," *Annual Reviews in Control*, 2020.

[30] N. M. A. A. Shannan, N. Z. Yahaya, and B. Singh, "Single-diode model and two-diode model of pv modules: A comparison," in *2013 IEEE International Conference on Control System, Computing and Engineering*. IEEE, 2013, pp. 210–214.

[31] K. Ishaque, Z. Salam, and H. Taheri, "Simple, fast and accurate two-diode model for photovoltaic modules," *Solar energy materials and solar cells*, vol. 95, no. 2, pp. 586–594, 2011.

[32] S. Bacha, I. Munteanu, A. I. Bratcu *et al.*, "Power electronic converters modeling and control," *Advanced textbooks in control and signal processing*, vol. 454, p. 454, 2014.

[33] R. Alba-Flores, D. Lucien, T. Kirkland, L. Snowden, and D. Herrin, "Design and performance analysis of three photovoltaic systems to improve solar energy collection," in *SoutheastCon 2018*. IEEE, 2018, pp. 1–4.

[34] N. Femia, G. Petrone, G. Spagnuolo, and M. Vitelli, "Optimization of perturb and observe maximum power point tracking method," *IEEE transactions on power electronics*, vol. 20, no. 4, pp. 963–973, 2005.

[35] J. D. Bastidas-Rodriguez, E. Franco, G. Petrone, C. A. Ramos-Paja, and G. Spagnuolo, "Maximum power point tracking architectures for photovoltaic systems in mismatching conditions: a review," *IET Power Electronics*, vol. 7, no. 6, pp. 1396–1413, 2014.

[36] Z. Salam, J. Ahmed, and B. S. Merugu, "The application of soft computing methods for mppt of pv system: A technological and status review," *Applied energy*, vol. 107, pp. 135–148, 2013.

[37] K. Ishaque and Z. Salam, "A review of maximum power point tracking techniques of pv system for uniform insolation and partial shading condition," *Renewable and Sustainable Energy Reviews*, vol. 19, pp. 475–488, 2013.

[38] M. Killi and S. Samanta, "Modified perturb and observe mppt algorithm for drift avoidance in photovoltaic systems," *IEEE transactions on Industrial Electronics*, vol. 62, no. 9, pp. 5549–5559, 2015.

[39] G.-C. Hsieh, H.-I. Hsieh, C.-Y. Tsai, and C.-H. Wang, "Photovoltaic power-increment-aided incremental-conductance mppt with two-phased tracking," *IEEE Transactions on Power Electronics*, vol. 28, no. 6, pp. 2895–2911, 2012.

[40] K. S. Tey and S. Mekhilef, "Modified incremental conductance mppt algorithm to mitigate inaccurate responses under fast-changing solar irradiation level," *Solar Energy*, vol. 101, pp. 333–342, 2014.

[41] W. Xiao and W. G. Dunford, "A modified adaptive hill climbing mppt method for photovoltaic power systems," in *2004 IEEE 35th annual power electronics specialists conference (IEEE Cat. No. 04CH37551)*, vol. 3.   Ieee, 2004, pp. 1957–1963.

[42] F. Liu, Y. Kang, Y. Zhang, and S. Duan, "Comparison of p&o and hill climbing mppt methods for grid-connected pv converter," in *2008 3rd IEEE Conference on Industrial Electronics and Applications*.   IEEE, 2008, pp. 804–807.

[43] H. Bounechba, A. Bouzid, K. Nabti, and H. Benalla, "Comparison of perturb & observe and fuzzy logic in maximum power point tracker for pv systems," *Energy Procedia*, vol. 50, no. 1, pp. 677–684, 2014.

[44] P. Q. Dzung, H. H. Lee, N. T. D. Vu *et al.*, "The new mppt algorithm using ann-based pv," in *International Forum on Strategic Technology 2010*.   IEEE, 2010, pp. 402–407.

[45] A. K. Rai, N. Kaushika, B. Singh, and N. Agarwal, "Simulation model of ann based maximum power point tracking controller for solar pv system," *Solar Energy Materials and Solar Cells*, vol. 95, no. 2, pp. 773–778, 2011.

[46] R. Khanaki, M. Radzi, and M. H. Marhaban, "Comparison of ann and p&o mppt methods for pv applications under changing solar irradiation," in *2013 IEEE Conference on Clean Energy and Technology (CEAT)*.   IEEE, 2013, pp. 287–292.

[47] S. Paul and J. Thomas, "Comparison of mppt using ga optimized ann employing pi controller for solar pv system with mppt using incremental conductance," in *2014 International Conference on Power Signals Control and Computations (EPSCICON)*.   IEEE, 2014, pp. 1–5.

[48] R. Zhang, S. Ong, and A. Y. Nee, "A simulation-based genetic algorithm approach for remanufacturing process planning and scheduling," *Applied Soft Computing*, vol. 37, pp. 521–532, 2015.

[49] B. Zhang, X. Li, and S. Wang, "A novel case adaptation method based on an improved integrated genetic algorithm for power grid wind disaster emergencies," *Expert Systems with Applications*, vol. 42, no. 21, pp. 7812–7824, 2015.

[50] R. Dou, C. Zong, and G. Nan, "Multi-stage interactive genetic algorithm for collaborative product customization," *Knowledge-Based Systems*, vol. 92, pp. 43–54, 2016.

[51] T. Baklacioglu, "Modeling the fuel flow-rate of transport aircraft during flight phases using genetic algorithm-optimized neural networks," *Aerospace Science and Technology*, vol. 49, pp. 52–62, 2016.

[52] R. Ramaprabha and B. Mathur, "Genetic algorithm based maximum power point tracking for partially shaded solar photovoltaic array," *International Journal of Research and Reviews in Information Sciences (IJRRIS) Vol*, vol. 2, 2012.

[53] J. Kennedy and R. Eberhart, "Particle swarm optimization," in *Proceedings of ICNN'95-International Conference on Neural Networks*, vol. 4. IEEE, 1995, pp. 1942–1948.

[54] U. Itkis, *Control systems of variable structure*. Halsted Press, 1976.

[55] J. Y. Hung, W. Gao, and J. C. Hung, "Variable structure control: A survey," *IEEE transactions on industrial electronics*, vol. 40, no. 1, pp. 2–22, 1993.

[56] C. Edwards and S. Spurgeon, *Sliding mode control: theory and applications*. Crc Press, 1998.

[57] W. Gao and J. C. Hung, "Variable structure control of nonlinear systems: A new approach," *IEEE transactions on Industrial Electronics*, vol. 40, no. 1, pp. 45–55, 1993.

[58] J.-J. Slotine and S. S. Sastry, "Tracking control of non-linear systems using sliding surfaces, with application to robot manipulators," *International journal of control*, vol. 38, no. 2, pp. 465–492, 1983.

[59] V. Utkin, J. Guldner, and M. Shijun, *Sliding mode control in electro-mechanical systems*. CRC press, 1999, vol. 34.

[60] I. Boiko and L. Fridman, "Analysis of chattering in continuous sliding-mode controllers," *IEEE transactions on automatic control*, vol. 50, no. 9, pp. 1442–1446, 2005.

[61] A. Levant, "Sliding order and sliding accuracy in sliding mode control," *International journal of control*, vol. 58, no. 6, pp. 1247–1263, 1993.

[62] ——, "Universal single-input-single-output (siso) sliding-mode controllers with finite-time convergence," *IEEE transactions on Automatic Control*, vol. 46, no. 9, pp. 1447–1451, 2001.

[63] K. J. Astrom and B. Wittenmark, "Adaptive control 2nd edition," *Addison-Wesley Pub Co.*, vol. 1994, 1994.

[64] V. I. Utkin, "Sliding modes in optimization and control problems," 1992.

[65] E. Dubrovskii and A. Kortnev, "Adaptative control systems with variable structure with bounded control actions, in the set of papers. systems with variable structure for flight automation," 1968.

[66] D. J. Perreault, K. Sato, R. L. Selders, and J. G. Kassakian, "Switching-ripple-based current sharing for paralleled power converters," *IEEE Transactions on Circuits and Systems I: Fundamental Theory and Applications*, vol. 46, no. 10, pp. 1264–1274, 1999.

[67] F. Plestan, Y. Shtessel, V. Bregeault, and A. Poznyak, "New methodologies for adaptive sliding mode control," *International journal of control*, vol. 83, no. 9, pp. 1907–1919, 2010.

[68] Y.-J. Huang, T.-C. Kuo, and S.-H. Chang, "Adaptive sliding-mode control for non-linearsystems with uncertain parameters," *IEEE Transactions on Systems, Man, and Cybernetics, Part B (Cybernetics)*, vol. 38, no. 2, pp. 534–539, 2008.

[69] H. Lee and V. I. Utkin, "Chattering suppression methods in sliding mode control systems," *Annual reviews in control*, vol. 31, no. 2, pp. 179–188, 2007.

[70] C. E. Hall and Y. B. Shtessel, "Sliding mode disturbance observer-based control for a reusable launch vehicle," *Journal of guidance, control, and dynamics*, vol. 29, no. 6, pp. 1315–1328, 2006.

[71] A. Bondarev, S. Bondarev, N. Kostyleva, and V. I. Utkin, "Sliding modes in systems with asymptotic state observers," *Avtomatika i Telemekhanika*, no. 6, pp. 5–11, 1985.

[72] Y.-H. Liu, C.-L. Liu, J.-W. Huang, and J.-H. Chen, "Neural-network-based maximum power point tracking methods for photovoltaic systems operating under fast changing environments," *Solar energy*, vol. 89, pp. 42–53, 2013.

[73] S. Saon, W. S. Chee *et al.*, "Development of optimum controller based on mppt for photovoltaic system during shading condition," *Procedia Engineering*, vol. 53, pp. 337–346, 2013.

[74] A. Tofighi and M. Kalantar, "Power management of pv/battery hybrid power source via passivity-based control," *Renewable Energy*, vol. 36, no. 9, pp. 2440–2450, 2011.

[75] D. R. Espinoza-Trejo, E. Bárcenas-Bárcenas, D. U. Campos-Delgado, and C. H. De Angelo, "Voltage-oriented input–output linearization controller as maximum power point tracking technique for photovoltaic systems," *IEEE Transactions on industrial electronics*, vol. 62, no. 6, pp. 3499–3507, 2014.

[76] D. Lalili, A. Mellit, N. Lourci, B. Medjahed, and C. Boubakir, "State feedback control and variable step size mppt algorithm of three-level grid-connected photovoltaic inverter," *Solar Energy*, vol. 98, pp. 561–571, 2013.

[77] C.-C. Chu and C.-L. Chen, "Robust maximum power point tracking method for photovoltaic cells: A sliding mode control approach," *Solar Energy*, vol. 83, no. 8, pp. 1370–1378, 2009.

[78] J. Ghazanfari and M. Maghfoori Farsangi, "Maximum power point tracking using sliding mode control for photovoltaic array," *Iranian Journal of Electrical and Electronic Engineering*, vol. 9, no. 3, pp. 189–196, 2013.

[79] V. Utkin, "Sliding mode control of dc/dc converters," *Journal of the Franklin Institute*, vol. 350, no. 8, pp. 2146–2165, 2013.

[80] H.-T. Yau and C.-L. Chen, "Fuzzy sliding mode controller design for maximum power point tracking control of a solar energy system," *Transactions of the Institute of Measurement and Control*, vol. 34, no. 5, pp. 557–565, 2012.

[81] P. A. O. Valencia and C. A. Ramos-Paja, "Sliding-mode controller for maximum power point tracking in grid-connected photovoltaic systems," *Energies*, vol. 8, no. 11, pp. 12 363–12 387, 2015.

[82] C.-S. Chiu, Y.-L. Ouyang, and C.-Y. Ku, "Terminal sliding mode control for maximum power point tracking of photovoltaic power generation systems," *Solar Energy*, vol. 86, no. 10, pp. 2986–2995, 2012.

[83] F. Attivissimo, A. Di Nisio, M. Savino, and M. Spadavecchia, "Uncertainty analysis in photovoltaic cell parameter estimation," *IEEE Transactions on Instrumentation and Measurement*, vol. 61, no. 5, pp. 1334–1342, 2012.

[84] T. Ahmad, S. Sobhan, and M. F. Nayan, "Comparative analysis between single diode and double diode model of pv cell: concentrate different parameters effect on its efficiency," *Journal of Power and Energy Engineering*, vol. 4, no. 3, pp. 31–46, 2016.

[85] S. Cuk and R. Middlebrook, "Advances in switched-mode power conversion part ii," *IEEE Transactions on Industrial Electronics*, no. 1, pp. 19–29, 1983.

[86] A. Noor, M. Abbas, K. S. Karimov *et al.*, "Non-inductive dc-dc regulated boost converter as battery charger for photovoltaic installation," in *2015 Power Generation System and Renewable Energy Technologies (PGSRET)*. IEEE, 2015, pp. 1–4.

[87] H. Gohar Ali, R. Vilanova Arbos, J. Herrera, A. Tobón, and J. Peláez-Restrepo, "Nonlinear sliding mode controller for photovoltaic panels with maximum power point tracking," *Processes*, vol. 8, no. 1, p. 108, 2020.

[88] H. Gohar Ali and R. V. Arbos, "Chattering free adaptive sliding mode controller for photovoltaic panels with maximum power point tracking," *Energies*, vol. 13, no. 21, p. 5678, 2020.

[89] J. J. Soon and K.-S. Low, "Photovoltaic model identification using particle swarm optimization with inverse barrier constraint," *IEEE Transactions on Power Electronics*, vol. 27, no. 9, pp. 3975–3983, 2012.

[90] D. G. Montoya, C. A. Ramos-Paja, and R. Giral, "Improved design of sliding-mode controllers based on the requirements of mppt techniques," *IEEE transactions on Power Electronics*, vol. 31, no. 1, pp. 235–247, 2015.